Quality & Quantity
https://doi.org/10.1007/s11135-024-02016-3

Mathematical model on the transmission dynamics of leptospirosis in human and animal population with optimal control strategies using real statistical data

Festus Abiodun Oguntolu[1] · Olumuyiwa James Peter[2,3] · Benjamin Idoko Omede[4] · Ghaniyyat Bolanle Balogun[5] · Tawakalt Abosede Ayoola[6]

Accepted: 24 October 2024

Abstract
Leptospirosis poses a significant public health challenge, with a growing incidence in both human and animal populations. The complex interplay between reservoir hosts, environmental factors, and human activities complicates efforts to curb the spread of the disease. Consequently, this paper presents a deterministic mathematical model for the transmission dynamics of leptospirosis within the intertwined human and animal populations. A comprehensive examination of the model revealed that the disease-free equilibrium is globally asymptotically stable when the basic reproduction number is below one. Utilizing center manifold theory, we demonstrated that the Leptospirosis model displays forward bifurcation. Consequently, the epidemiological significance of this forward bifurcation suggests that eradicating leptospirosis from the community is feasible, provided the reproduction number remains below one. We conducted a sensitivity analysis on the basic reproduction number of Leptospirosis to identify parameters that contribute positively to the disease's spread. Furthermore, We validated our Leptospirosis model by fitting it with confirmed cases reported in Kerala State, India, covering the period from January 2021 to December 2022. This calibration process ensures the model's accuracy and reliability in reflecting real-world epidemiological dynamics within the specified region and timeframe. In addition, we enhanced the Leptospirosis model by incorporating three time-dependent control measures. These controls encompass the vaccination of animals, environmental sanitation, and preventive actions such as using hand gloves and goggles when handling animals, as well as wearing rubber boots during periods of flooding or heavy rainfall. Results obtained from numerical simulations indicate that implementing the vaccination of animals as a standalone control strategy has no discernible effect on the number of infected humans or the bacteria population. However, when the three time-dependent control measures are combined, there is a substantial and meaningful impact on reducing the number of infected humans, infected animals, and the overall bacteria population within a relatively short timeframe. This underscores the effectiveness of the integrated approach in mitigating the spread of leptospirosis across both human and animal populations.

Keywords Leptospirosis · Basic reproduction number · Stability · Sensitivity analysis · Bifurcation

Extended author information available on the last page of the article

Published online: 07 December 2024

Mathematics Subject Classification 92B05 · 92D30 · 92-10 · 34D20

1 Introduction

Leptospirosis, traditionally considered one of the most overlooked tropical diseases, is a zoonotic and water-borne illness caused by spirochete bacteria known as *Leptospira* Spp., belonging to the genus *Leptospira* (Esteves et al. 2018; Chatterjee et al. 2017; Md-Lasim et al. 2021). The genus *Leptospira* encompasses 20 species, further classified into 24 serogroups, with over 300 serovars (Picardeau 2013). Annually, this disease accounts for over 1 million new and severe cases, leading to almost 60,000 deaths globally (Thibeaux et al. 2018). The reproduction of *Leptospira* typically takes place in the renal tubules of infected mammals (Thibeaux et al. 2018; Evangelista and Coburn 2010). Subsequently, these bacteria are expelled into the environment through urine, posing a risk of infecting other organisms. The average incubation period is 1 or 2 weeks, with a range spanning from 2 days to 30 days (Costa et al. 2015; Bierque et al. 2020). Infections with *Leptospira* typically arise through skin abrasions, wounds, or mucosal contact, facilitating the organism's entry into the bloodstream and subsequent dissemination to the kidneys (Faisal et al. 2012). Direct transmission to humans can occur through the handling of infected animals, rendering leptospirosis an occupational risk for individuals regularly in contact with animals. This includes professions like livestock producers, workers in abattoirs, veterinarians, hunters, game managers, animal control workers, and scientists (López-Robles et al. 2021; Rahman et al. 2018; Sykes et al. 2022). More frequently, leptospirosis is contracted indirectly through exposure to contaminated water or soil (Bierque et al. 2020; Sykes et al. 2022). Consequently, individuals who closely interact with soil and water systems, such as sewage and waste workers, those in construction, the military, aquaculture workers, and farmers, face an occupational risk of leptospirosis (Hartskeerl et al. 2011; Narita et al. 2005). Moreover, this disease poses a growing environmental hazard for outdoor enthusiasts engaging in activities like kayaking, swimming, fishing, and more (Mwachui et al. 2015; Pappas et al. 2008).

Rain and floods are recognized as primary risk factors for leptospirosis, with documented outbreaks occurring worldwide in the aftermath of extreme weather events. Instances of such outbreaks have been reported in various locations, including Brazil, Guyana, Italy, New Caledonia, Nicaragua, the Philippines, and the United States (Liverpool et al. 2008; Al-shere et al. 2012). Animal infections commonly occur either through direct contact with *Leptospira*-contaminated urine or indirectly through interaction with water and/or soil that is contaminated with the bacterium (Guernier et al. 2018). Additionally, given that the bacterium has been identified in the reproductive fluids of bovines, equines, ovines, and swines, the possibility of sexual transmission should not be disregarded (Loureiro and Lilenbaum 2020). Significant populations of rodents, farm animals, and dogs can harbor *Leptospira* within their kidneys, leading to the shedding of the bacterium in urine and contributing to its spread in the environment (Bradley and Lockaby 2023). In cases where *Leptospira* persists in the renal and urinary systems and is subsequently shed by animals, the bacteria have the capability to survive under optimal environmental conditions for several months, lasting up to a year (Sykes et al. 2022). Human leptospirosis is predominantly characterized by acute clinical features commonly referred to as Weil's disease, which includes intense symptoms such as fever, icterus, renal insufficiency, and a risk of mortality (O'Toole et al. 2015). Domestic animals, particularly dogs, may also exhibit this acute and potentially lethal infection akin to Weil's disease. In such cases, substantial renal damage can occur. Horses, on the other hand, may manifest

recurrent uveitis and a decrease in athletic performance (Verma et al. 2015; Hamond et al. 2012). In bovines, as well as in other ruminants, the acute and severe form of leptospirosis is infrequent and often linked to sporadic outbreaks in calves due to incidental strains (Loureiro and Lilenbaum 2020). The prevailing presentation of animal leptospirosis is, indeed, the subclinical and silent chronic form, which is frequently overlooked (Adler 2014). In this particular presentation, reproductive signs take precedence. The chronic form of leptospirosis, marked by *Leptospira* colonization of the reproductive tract, results in significant reproductive disorders, ultimately causing substantial economic losses (Mori et al. 2017).

Treatment for leptospirosis primarily involves the use of various antibiotics, which can be administered either orally or intravenously (Yaakob et al. 2015). Commonly employed antibiotics include tetracyclines, penicillin, and ceftriaxone (Brett-Major and Coldren 2012). Penicillin is the most frequently used antibiotic in the treatment of leptospirosis (Charan et al. 2013). Early administration of these antibiotics is crucial, significantly reducing the risk of developing severe forms like Weil's disease and decreasing mortality rates (Tubiana et al. 2013). In cases where leptospirosis progresses to Weil's disease, intensive care treatment may be necessary, involving interventions such as hemodialysis and blood transfusions. The management of severe pulmonary hemorrhages often requires mechanical ventilation (Goarant 2016). Designing a vaccine for leptospirosis remains a significant challenge, persisting since its discovery in 1886. The complexity arises from the existence of more than 230 pathogenic strains, and the intricacies of the infection's pathogenesis are not fully understood. The diversity of distinct strains circulating globally makes it impractical to develop a single universal vaccine (Xu and Ye 2018). Vaccines containing inactivated whole cells (bacterins) have been in use for over a century and are presently the only licensed vaccines for leptospirosis control (Vernel-Pauillac and Werts 2018; Ido et al. 1916). While primarily intended for animal use, in countries like France, Cuba, China, and Japan, bacterins have been approved for use in human populations at risk (Adler and de la Peña Moctezuma 2010).

Over the years, mathematical modeling has played a crucial role in studying the transmission dynamics of infectious diseases. While there has been a comprehensive application of mathematical models in this context, Several models have been specifically designed to study the transmission dynamics of leptospirosis. For instance, Aslan and Lenhart (2020) proposed a mathematical model to assess cost-effectiveness and facilitate the prompt identification of leptospirosis in humans. They devised a computational algorithm that incorporates stochastic elements, employing Markov-cycle trees and Monte Carlo simulations to simulate individuals entering a hospital under suspicion of leptospirosis. Antima and Banerjee (2023) designed a mathematical model to depict the transmission dynamics of leptospirosis in India. Their model includes a temperature-dependent square growth rate of Leptospira, providing a more precise representation of leptospirosis dynamics by considering the intricate relationship between temperature and infection rate. Khan et al. (2016) presented a mathematical model for leptospirosis diseases incorporating a saturated incidence rate. Chadsuthi et al. (2022) formulated a kinetic model for animal leptospirosis, integrating both antibody (exposure marker) and infection dynamics. This model concurrently tracks seroconversion and infection statuses of leptospirosis in a herd population. The states of infection and antibody classes within the population are expressed as a function of the basic reproduction number, facilitating the correlation between the number of infectious individuals (epizootic size) and the prevalence of antibody-positive individuals. Aslan et al. (2021) constructed an age-structured model with impulse actions to analyze leptospirosis in livestock cattle. The model incorporates vaccination and cattle replacement as impulse actions, allowing for an examination of their effects and a comparison of the schedules for implementing these actions. Sadiq et al. (2014) investigated a leptospirosis epidemic model with a non-linear saturated incidence, employing optimal control techniques to devise strategies for eradicating the

infection within the human population. Engida et al. (2022) developed and examined a mathematical model describing the transmission dynamics of leptospirosis disease in both human and rodent populations. Their analysis uncovered a forward bifurcation in the model. Additionally, the results from numerical simulations indicated that reducing the rodent population through appropriate intervention mechanisms plays a significant role in mitigating the spread of disease infection in the overall population.

To the best of our knowledge, this is the first study on the dynamics of Leptospirosis which considers both human and animal population with optimal control strategies by incorporating a broader perspective on the animal population, encompassing more than just rodents. Additionally, we incorporated animal-to-animal transmission into our analysis and conducting a thorough examination of the model. Furthermore, we introduced three time-dependent control measures. These measures involve the vaccination of animals, environmental sanitation to diminish the concentration of Leptospira, and preventative actions such as the use of hand gloves and goggles when handling animals, along with wearing rain boots during periods of flooding or heavy rainfall. The rest of the paper is organized as follows: the model formulation and basic properties of the model are described in Sect. 2, the model analysis in Sect. 3, the optimal control analysis in Sect. 4, and Sect. 5 is the concluding remarks.

2 Model formulation

The Leptospirosis model is divided into three population namely; the human population, the animal population, and the bacteria population. The total human population at time t, denoted by $N_H(t)$, is sub-divided into five mutually exclusive compartments of susceptible humans $S_H(t)$, exposed humans $E_H(t)$, infected humans $I_H(t)$, treated humans $T_H(t)$, and recovered humans $R_H(t)$. So that

$$N_H(t) = S_H(t) + E_H(t) + I_H(t) + T_H(t) + R_H(t).$$

The total animal (vector) population at time t, denoted by $N_V(t)$, is sub-divided into four mutually exclusive compartments of susceptible vectors $S_V(t)$, exposed vectors $E_V(t)$, infected vectors $I_V(t)$, and recovered vectors $R_V(t)$. So that

$$N_V(t) = S_V(t) + E_V(t) + I_V(t) + R_V(t).$$

The population of the susceptible humans $S_H(t)$ is generated by the recruitment of individuals into the population either by birth or migration at the rate Π_H. Susceptible humans acquires Leptospirosis following and effective contact with infected animals with Leptospirosis or Leptospirosis bacteria in the environment at the rate λ_H, given by,

$$\lambda_H = \frac{\alpha_H I_V}{N_H} + \frac{\alpha_{HB} B}{K + B}.$$

where α_H is the transmission probability from infected animals to susceptible humans, α_{HB} is the transmission probability from contaminated environment with Leptospirosis bacteria to susceptible humans, and K is the carrying capacity (i.e. the concentration of the bacteria in the environment) of the leptospirosis bacteria. The susceptible humans that come in contact with infected animals or contaminated environment with Leptospirosis progressed to the exposed class at the rate λ_H, and then progressed to being infected at the rate γ. The infected humans progressed to the treated class at the rate σ, and the disease-induced death rate of infected humans is given by δ_H. Natural death occurs in all human sub-population

at the rate θ_H. Treated individuals may die from the disease at the rate $\phi\delta_H$ (where ϕ is the parameter that accounts for death in the treatment class), and ε is the recovery rate of treated individuals. Recovered humans from Leptospirosis becomes susceptible again at the rate ρ_H.

The population of the susceptible vectors is generated by the recruitment rate Π_V. The susceptible vectors acquires Leptospirosis following and effective contact with infected vectors or Leptospirosis bacteria from contaminated environment at the rate λ_V, given by

$$\lambda_V = \frac{\alpha_V I_V}{N_V} + \frac{\alpha_{VB} B}{K + B}.$$

where α_V is the transmission probability from infected vectors to susceptible vectors, α_{VB} is the transmission probability from contaminated environment with Leptospirosis bacteria to susceptible vectors, and K is the carrying capacity of the bacteria. The susceptible vectors that come in contact with infected vectors or contaminated environment progressed to the exposed class at the rate λ_V, and then progressed to being infected at the rate ψ. Infected vectors recovers from Leptospirosis at the rate τ, and dies from the disease at the rate δ_V. The natural death rate of vectors is the same for all the animal sub-population at the rate θ_V. Recovered vectors from Leptospirosis becomes susceptible again at the rate ρ_V.

The bacteria population denoted by $B(t)$, is generated by the shedding of Leptospirosis in the environment by infected animals and infected humans at the rates ω_1 and ω_2 respectively. The population of the bacteria is decreased by the clearance of the bacteria in the environment at the rate θ_B. The description of the model variables and parameters is given in Table 1, while Fig. 1 represent the model's flow chart.

Base on the above formulations and assumptions the Leptospirosis model is governed by the system of non-linear differential equations given below

$$\begin{aligned}
\frac{dS_H}{dt} &= \Pi_H - \lambda_H S_H - \theta_H S_H + \rho_H R_H \\
\frac{dE_H}{dt} &= \lambda_H S_H - \left(\gamma + \theta_H\right) E_H \\
\frac{dI_H}{dt} &= \gamma E_H - \left(\sigma + \delta_H + \theta_H\right) I_H \\
\frac{dT_H}{dt} &= \sigma I_H - \left(\varepsilon + \phi\delta_H + \theta_H\right) T_H \\
\frac{dR_H}{dt} &= \varepsilon T_H - \left(\rho_H + \theta_H\right) R_H \\
\frac{dS_V}{dt} &= \Pi_V - \lambda_V S_V - \theta_V S_V + \rho_V R_V \\
\frac{dE_V}{dt} &= \lambda_V S_V - \left(\psi + \theta_V\right) E_V \\
\frac{dI_V}{dt} &= \psi E_V - \left(\tau + \delta_V + \theta_V\right) I_V \\
\frac{dR_V}{dt} &= \tau I_V - \left(\rho_V + \theta_V\right) R_V \\
\frac{dB}{dt} &= \omega_1 I_V + \omega_2 I_H - \theta_B B,
\end{aligned} \tag{1}$$

where

Table 1 Description of the model variables and parameters

Variable	Description
S_H	Population of susceptible humans
E_H	Population of exposed humans to leptospirosis
I_H	Population of infected humans with leptospirosis
T_H	Population of treated humans with leptospirosis
R_H	Population of recovered humans from leptospirosis
S_V	Population of susceptible vectors
E_V	Population of exposed vectors to leptospirosis
I_V	Population of infected vectors with leptospirosis
R_V	Population of recovered vectors with leptospirosis
B	Bacteria population
Parameter	Description
$\Pi_H(\Pi_V)$	Recruitment rate for humans (vectors)
α_H	Effective contact rate between susceptible humans and infected vectors
α_V	Effective contact rate between susceptible vectors and infected vectors
α_{HB}	Effective contact rate between susceptible humans and bacteria in the environment
α_{VB}	Effective contact rate between susceptible vectors and bacteria in the environment
θ_H	Human natural death rate
θ_V	Vector natural death rate
θ_B	Clearance of bacteria from the environment
γ	Progression rate from $E_H(t)$ class to $I_H(t)$ class
σ	Treatment rate of infected humans
δ_H	Disease-induced death rate for humans
δ_V	Disease-induced death rate for vectors
$\rho_H(\rho_V)$	The rate at which recovered humans (vectors) become susceptible again
ϕ	Modification parameter that accounts for reduction in disease-induced death in the treatment class
ε	Recovery rate of treated humans
τ	Recovery rate of infected animals
ψ	Progression rate from E_V class to I_V class
ω_1	Rate of shedding Leptospirosis bacteria in the environment from infected vectors
ω_2	Rate of shedding Leptospirosis bacteria in the environment from infected humans
K	Carrying capacity

$$\lambda_H = \frac{\alpha_H I_V}{N_H} + \frac{\alpha_{HB} B}{K + B}, \quad \textit{and} \quad \lambda_V = \frac{\alpha_V I_V}{N_V} + \frac{\alpha_{VB} B}{K + B}.$$

2.1 Basic properties of the model

2.1.1 Positivity of solution

For the Leptospirosis model (1) to be biologically meaningful, the solution of the system must be non-negative for all values of time t. Thus, it is necessary to show that all

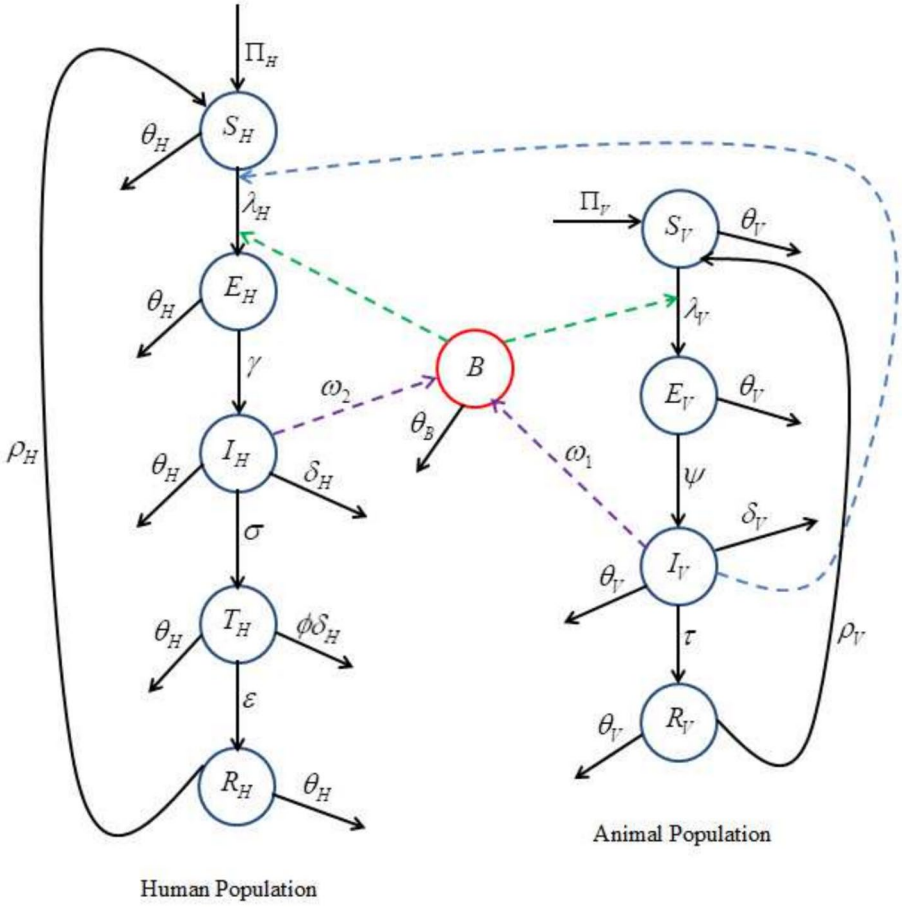

Fig. 1 Flowchart of the Leptospirosis model

the state variables of the Leptospirosis model (1) are positive for all time $t > 0$, in the feasible region $\mathcal{D}$, given by

$$\mathcal{D} = \mathcal{D}_H \cup \mathcal{D}_V \cup \mathcal{D}_B \subset \mathfrak{R}_+^5 \times \mathfrak{R}_+^4 \times \mathfrak{R}_+^1. \tag{2}$$

where

$$\mathcal{D}_H = \left\{ \left(S_H, E_H, I_H, T_H, R_H\right) \in \mathfrak{R}_+^5 : N_H \leq \frac{\Pi_H}{\theta_H} \right\},$$
$$\mathcal{D}_V = \left\{ \left(S_V, E_V, I_V, R_V\right) \in \mathfrak{R}_+^4 : N_V \leq \frac{\Pi_V}{\theta_V} \right\},$$

and

$$\mathcal{D}_B = \left\{ B \in \mathfrak{R}_+^1 : B \leq \frac{\omega^*}{\theta_B} \left(\frac{\Pi_V}{\theta_V} + \frac{\Pi_H}{\theta_H} \right) \right\}.$$

Theorem 1 *Let the initial data for the Leptospirosis model* (1) *be* $S_H(0) > 0$, $E_H(0) \geq 0$, $I_H \geq 0$, $T_H(0) \geq 0$, $R_H(0) \geq 0$, $S_V(0) \geq 0$, $E_V(0) \geq 0$, $I_V(0) \geq 0$, $R_V(0) \geq 0$, *and* $B \geq 0$. *Then the solution* $\left(S_H, E_H, I_H, T_H, R_H, S_V, E_V, I_V, R_V, B\right)$ *of the Leptospirosis model* (1) *are non-negative for all time* $t > 0$.

Proof Let $t_f = \sup\left\{t > 0 : \left(S_H > 0, E_H > 0, I_H > 0, T_H > 0, R_H > 0, S_V > 0, E_V > 0, I_V > 0, R_V > 0, B > 0\right) \in [0, t]\right\}$. Thus, $t_f > 0$. From the first equation of Leptospirosis model system (1), we have

$$\frac{dS_H}{dt} = \Pi_H - \lambda_H S_H - \theta_H S_H + \rho_H R_H$$

Solving the above equation, we obtained

$$\frac{d}{dt}\left\{S_H(t)\left[\exp\left(\int_0^t \lambda_H(y)dy + \theta_H t\right)\right]\right\} = \left(\Pi_H + \rho_H R_H\right)\exp\left(\int_0^t \lambda_H(y)dy + \theta_H t\right)$$

Integrating the above equation at the range $[0, t_f]$, we obtained

$$\begin{aligned}&\left\{S_H(t)\exp\left[\int_0^{t_f} \lambda_H(y)dy + \theta_H t_f\right]\right\} - S_H(0)\\ &\quad = \left(\Pi_H + \rho_H R_H\right)\int_0^{t_f}\exp\left[\int_0^z \lambda_H(y)dy + \theta_H z\right]dz\end{aligned}$$

So that

$$\begin{aligned}S_H(t) = S_H(0)\exp\left[-\left(\int_0^{t_f} \lambda_H(y)dy + \theta_H t_f\right)\right] + \exp\left[-\left(\int_0^{t_f} \lambda_H(y)dy + \theta_H t_f\right)\right]\times\\ \left(\Pi_H + \rho_H R_H\right)\int_0^{t_f}\exp\left[\int_0^z \lambda_H(y)dy + \theta_H z\right]dz > 0\end{aligned}$$

Similarly, it can be shown that $E_H > 0$, $I_H > 0$, $T_H > 0$, $R_H > 0$, $S_V > 0$, $E_V > 0$, $I_V > 0$, $R_V > 0$, $B > 0$. □

2.1.2 Invariant region

Lemma 1 *The region* $\mathcal{D} = \mathcal{D}_H \cup \mathcal{D}_V \cup \mathcal{D}_B \subset \mathfrak{R}_+^5 \times \mathfrak{R}_+^4 \times \mathfrak{R}_+^1$ *is positively invariant and attracts all solution in* $\mathfrak{R}_+^{10}$.

Proof By adding the equations of the human, animal and bacteria compartments of the Leptospirosis model (1). The rate of change of the human, animal and bacteria population are given by

$$\begin{aligned}\frac{dN_H}{dt} &= \Pi_H - \theta_H N_H - \delta_H I_H - \phi\delta_H T_H,\\ \frac{dN_V}{dt} &= \Pi_V - \theta_V N_V - \delta_V I_V,\end{aligned}$$

and

$$\frac{dB}{dt} = \omega_1 I_V + \omega_2 I_H - \theta_B B.$$

We have that

$$\begin{aligned}\frac{dN_H}{dt} \leq & \Pi_H - \theta_H N_H,\\ \frac{dN_V}{dt} \leq & \Pi_V - \theta_V N_V,\end{aligned}$$

and

$$\frac{dB}{dt} \leq \omega^* \left(\frac{\Pi_V}{\theta_V} + \frac{\Pi_H}{\theta_H}\right) - \theta_B B.$$

where $\omega^* = \max\left(\omega_1, \omega_2\right)$.

A standard comparison theorem described in Lakshmikantham et al. (1989) can be used to show that

$$\begin{aligned}N_H(t) \leq & N_H(0)e^{-\theta_H t} + \frac{\Pi_H}{\theta_H}\left(1 - e^{-\theta_H t}\right),\\ N_V(t) \leq & N_V(0)e^{-\theta_V t} + \frac{\Pi_V}{\theta_V}\left(1 - e^{-\theta_V t}\right),\end{aligned}$$

and

$$B(t) \leq B(0)e^{-\theta_B t} + \frac{\omega^*}{\theta_B}\left(\frac{\Pi_V}{\theta_V} + \frac{\Pi_H}{\theta_H}\right)\left(1 - e^{-\theta_B t}\right).$$

It follows that if $N_H(0) \leq \frac{\Pi_H}{\theta_H}$, $N_V(0) \leq \frac{\Pi_V}{\theta_V}$, and $B(0) \leq \frac{\omega^*}{\theta_B}\left(\frac{\Pi_V}{\theta_V} + \frac{\Pi_H}{\theta_H}\right)$, then $N_H(t) \leq \frac{\Pi_H}{\theta_H}$, $N_V(t) \leq \frac{\Pi_V}{\theta_V}$, and $B(t) \leq \frac{\omega^*}{\theta_B}\left(\frac{\Pi_V}{\theta_V} + \frac{\Pi_H}{\theta_H}\right)$. Thus, the region $\mathcal{D}$ is positively-invariant and attracts all the solutions in $\mathfrak{R}^{10}_+$. Therefore, the Leptospirosis model (1) is biologically and mathematically well-posed in the region $\mathcal{D}$. Hence, it is satisfactory to examine the dynamics of the Leptospirosis model (1) in the region $\mathcal{D}$ (Hethcote 2000). □

3 Model analysis

3.1 Disease-free equilibrium

The disease-free equilibrium is a steady state in which there is absence of Leptospirosis in the population. This is achieved by setting the infected compartments to zero (that is $E_H = I_H = T_H = E_V = I_V = B = 0$) and equating the right hand side of the Leptospirosis model (1) to zero. Thus, the disease-free equilibrium of the Leptospirosis model is given by

$$\xi_0 = \left(S_H^*, E_H^*, I_H^*, T_H^*, R_H^*, S_V^*, E_V^*, I_V^*, R_V^*, B^*\right) = \left(\frac{\Pi_H}{\theta_H}, 0, 0, 0, 0, \frac{\Pi_V}{\theta_V}, 0, 0, 0, 0\right) \quad (3)$$

3.2 Basic reproduction number

The basic reproduction number, denoted as ($\mathcal{R}_0$), plays a crucial role as a threshold parameter governing disease spread within a population. It characterizes the stability of the disease-free equilibrium (DFE) in a model, depicting the pinnacle and ultimate scale of an epidemic (Van den Driessche and Watmough 2002). The basic reproduction number is defined as the expected number of secondary infections resulting from the introduction of a single infectious individual into a fully susceptible population. Its calculation involves employing the next generation operator method outlined in Van den Driessche and Watmough (2002). This method utilizes matrices representing the new infection ($\mathscr{F}$) and the remaining transition terms ($\mathscr{V}$), respectively. The matrices $\mathscr{F}$ and $\mathscr{V}$ are evaluated at the disease-free equilibrium, and are given by

$$\mathscr{F} = \begin{bmatrix} 0 & 0 & 0 & 0 & \alpha_H & \frac{\alpha_{HB}\Pi_H}{\theta_H K} \\ 0 & 0 & 0 & 0 & 0 & 0 \\ 0 & 0 & 0 & 0 & 0 & 0 \\ 0 & 0 & 0 & 0 & \alpha_V & \frac{\alpha_{VB}\Pi_V}{\theta_V K} \\ 0 & 0 & 0 & 0 & 0 & 0 \\ 0 & 0 & 0 & 0 & 0 & 0 \end{bmatrix}, \text{and}$$

$$\mathscr{V} = \begin{bmatrix} (\gamma+\theta_H) & 0 & 0 & 0 & 0 & 0 \\ -\gamma & (\sigma+\delta_H+\theta_H) & 0 & 0 & 0 & 0 \\ 0 & -\sigma & (\varepsilon+\phi\delta_H+\theta_H) & 0 & 0 & 0 \\ 0 & 0 & 0 & (\psi+\theta_V) & 0 & 0 \\ 0 & 0 & 0 & -\psi & (\tau+\delta_V+\theta_V) & 0 \\ 0 & -\omega_2 & 0 & 0 & -\omega_1 & \theta_B \end{bmatrix}$$

we have that

$$\mathscr{F}\mathscr{V}^{-1} = \begin{bmatrix} \frac{\alpha_{HB}\Pi_H\omega_2\gamma}{\theta_H\theta_B K g_1 g_2} & \frac{\alpha_{HB}\Pi_H\omega_2}{\theta_H\theta_B K g_2} & 0 & \frac{\alpha_H\psi}{g_5 g_6} + \frac{\alpha_{HB}\Pi_H\omega_1\psi}{\theta_H\theta_B K g_5 g_6} & \frac{\alpha_H}{g_6} + \frac{\alpha_{HB}\Pi_H\omega_1}{\theta_H\theta_B K g_6} & \frac{\alpha_{HB}\Pi_H}{\theta_H\theta_B K} \\ 0 & 0 & 0 & 0 & 0 & 0 \\ 0 & 0 & 0 & 0 & 0 & 0 \\ \frac{\alpha_{VB}\Pi_V\omega_2\gamma}{\theta_V\theta_B K g_1 g_2} & \frac{\alpha_{VB}\Pi_V\omega_2}{\theta_V\theta_B K g_2} & 0 & \frac{\alpha_V\psi}{g_5 g_6} + \frac{\alpha_{VB}\Pi_V\omega_1\psi}{\theta_V\theta_B K g_5 g_6} & \frac{\alpha_V}{g_6} + \frac{\alpha_{VB}\Pi_V\omega_1}{\theta_V\theta_B K g_6} & \frac{\alpha_{VB}\Pi_V}{\theta_V\theta_B K} \\ 0 & 0 & 0 & 0 & 0 & 0 \\ 0 & 0 & 0 & 0 & 0 & 0 \end{bmatrix}$$

where

$g_1 = \gamma + \theta_H$, $g_2 = \sigma + \delta_H + \theta_H$, $g_3 = \varepsilon + \phi\delta_H + \theta_H$, $g_4 = \rho + \theta_H$, $g_5 = \psi + \theta_V$, and $g_6 = \tau + \delta_V + \theta_V$.

Hence, it follows from (Van den Driessche and Watmough 2002) that $\mathcal{R}_0 = \rho(\mathscr{F}\mathscr{V}^{-1})$, where ρ is the spectral radius or dominant eigenvalues of the matrix $\mathscr{F}\mathscr{V}^{-1}$.

The characteristic polynomial of the matrix $\mathscr{F}\mathscr{V}^{-1}$, is given by

$$\lambda^4\left(\lambda^2 - D_1\lambda - D_2\right) = 0 \tag{4}$$

where

$$D_1 = \frac{\alpha_V \psi \theta_H \theta_V \theta_B K g_1 g_2 + \alpha_{VB} \psi \omega_1 \Pi_V \theta_H g_1 g_2 + \alpha_{HB} \gamma \omega_2 \Pi_H \theta_V g_5 g_6}{\theta_H \theta_V \theta_B K g_1 g_2 g_5 g_6}, \text{ and}$$

$$D_2 = \frac{\left(\alpha_{VB} \alpha_H \Pi_V \theta_H - \alpha_{HB} \alpha_V \Pi_H \theta_V\right) \gamma \psi \omega_2}{\theta_H \theta_V \theta_B K g_1 g_2 g_5 g_6}$$

The quadratic equation associated to the above characteristic polynomial in () is $\mathscr{M}(\lambda) = \left(\lambda^2 - D_1 \lambda - D_2\right)$, with $D_1 > 0$, $D_2 > 0$. Thus, the solution of $\mathscr{M}(\lambda) = 0$ gives a unique positive root, which is the dominant eigenvalue of the basic reproduction number of the Leptospirosis model, given by

$$\mathcal{R}_0 = \frac{1}{2}\left(D_1 + \left(D_1^2 + 4D_2\right)^{\frac{1}{2}}\right) \tag{5}$$

Furthermore, $\mathscr{M}(0) = -D_2 < 0$, and $\mathscr{M}(1) = 1 - (D_1 + D_2)$. We define $\mathcal{R}_0^L = D_1 + D_2$, given by

$$\mathcal{R}_0^L = \frac{\alpha_V \psi}{g_5 g_6} + \frac{\alpha_{VB} \psi \omega_1 \Pi_V}{\theta_V \theta_B K g_5 g_6} + \frac{\alpha_{HB} \gamma \omega_2 \Pi_H}{\theta_H \theta_B K g_1 g_2} + \frac{\left(\alpha_{VB} \alpha_H \Pi_V \theta_H - \alpha_{HB} \alpha_V \Pi_H \theta_V\right) \gamma \psi \omega_2}{\theta_H \theta_V \theta_B K g_1 g_2 g_5 g_6}. \tag{6}$$

That is

$$\mathcal{R}_0^L = \mathcal{R}_0^V + \mathcal{R}_0^{VB} + \mathcal{R}_0^{HB} + \mathcal{R}_0^{VHB}$$

Where

$\mathcal{R}_0^V$ is the contribution from vector to vector transmission, $\mathcal{R}_0^{VB}$ is the contribution from environment to vector transmission, $\mathcal{R}_0^{HB}$ is the contribution from environment to human transmission, and $\mathcal{R}_0^{VHB}$ is the contribution from environment to vector to human transmission.

Again, from the relation $\mathscr{M}(1) = 1 - \mathcal{R}_0^L$, we have the following observation;

(i) When $\mathcal{R}_0^L = 1$ then $\mathscr{M}(1) = 0$, thus the positive root of the equation $\mathscr{M}(\lambda) = 0$ is one $\left(\mathcal{R}_0 = 1\right)$.
(ii) When $\mathcal{R}_0^L < 1$ then $\mathscr{M}(1) > 0$, so the positive root of the equation lies between 0 and 1 as $\mathscr{M}(0) < 0$, thus $\mathcal{R}_0 < 1$.
(iii) When $\mathcal{R}_0^L > 1$ then $\mathscr{M}(1) < 0$ again $\mathscr{M}(0) < 0$, so the positive root $\mathscr{M}(\lambda) = 0$ is greater than one (that is $\mathcal{R}_0 > 1$).

Hence, from the above observations, one can conclude that $\mathcal{R}_0^L = 1(< 1, > 1)$ if and only if $\mathcal{R}_0 = 1(< 1, > 1)$. Since the two threshold parameter $\mathcal{R}_0$ and $\mathcal{R}_0^L$ are equivalent (Jose et al. 2023; Omede et al. 2023). We shall be using $\mathcal{R}_0^L$ as the Leptospirosis basic reproduction number in the subsequent sections.

3.3 Local stability of the disease-free equilibrium

Theorem 2 *The disease-free equilibrium* (ξ_0) *of the Leptospirosis model* (1) *is locally asymptotically stable if* $\mathcal{R}_0^L < 1$, *and unstable if* $\mathcal{R}_0^L > 1$.

Proof The local stability of the disease-free equilibrium is analyzed by obtaining the Jacobian matrix of the Leptospirosis model (1), evaluated at the disease-free equilibrium (ξ_0), given by

$$J(\xi_0) = \begin{bmatrix} -\theta_H & 0 & 0 & 0 & \rho_H & 0 & 0 & -\alpha_H & 0 & -\frac{\alpha_{HB}\Pi_H}{\theta_H K} \\ 0 & -g_1 & 0 & 0 & 0 & 0 & 0 & \alpha_H & 0 & \frac{\alpha_{HB}\Pi_H}{\theta_H K} \\ 0 & \gamma & -g_2 & 0 & 0 & 0 & 0 & 0 & 0 & 0 \\ 0 & 0 & \sigma & -g_3 & 0 & 0 & 0 & 0 & 0 & 0 \\ 0 & 0 & 0 & \varepsilon & -g_4 & 0 & 0 & 0 & 0 & 0 \\ 0 & 0 & 0 & 0 & 0 & -\theta_V & 0 & -\alpha_V & \rho_V & -\frac{\alpha_{VB}\Pi_V}{\theta_V K} \\ 0 & 0 & 0 & 0 & 0 & 0 & -g_5 & \alpha_V & 0 & \frac{\alpha_{VB}\Pi_V}{\theta_V K} \\ 0 & 0 & 0 & 0 & 0 & 0 & \psi & -g_6 & 0 & 0 \\ 0 & 0 & 0 & 0 & 0 & 0 & 0 & \tau & -g_7 & 0 \\ 0 & 0 & \omega_2 & 0 & 0 & 0 & 0 & \omega_1 & 0 & -\theta_B \end{bmatrix}$$

where

$g_1 = \gamma + \theta_H$, $g_2 = \sigma + \delta_H + \theta_H$, $g_3 = \varepsilon + \phi\delta_H + \theta_H$, $g_4 = \rho_H + \theta_H$, $g_5 = \psi + \theta_V$, $g_6 = \tau + \delta_V + \theta_V$, and $g_7 = \rho_V + \theta_V$.

The eigenvalues of the Jacobian matrix $J(\xi_0)$ above are $\lambda_1 = -\theta_H$, $\lambda_2 = -\theta_V$, $\lambda_3 = -g_3$, $\lambda_4 = -g_4$, $\lambda_5 = -g_7$ and the roots of the characteristic polynomial given below

$$Q(\lambda) = \lambda^5 + m_1\lambda^4 + m_2\lambda^3 + m_3\lambda^2 + m_4\lambda + m_5 \tag{7}$$

where

$$\begin{aligned}
m_1 &= g_1 + g_2 + g_5 + g_6 + \theta_B, \\
m_2 &= g_1(g_2 + g_5 + g_6 + \theta_B) + g_2(g_5 + g_6 + \theta_B) + g_5(g_6 + \theta_B) + g_6\theta_B - \alpha_V\psi, \\
m_3 &= g_1g_2(g_5 + g_6 + \theta_B) + g_1g_5(g_6 + \theta_B) + g_6\theta_B(g_1 + g_2 + g_5) \\
&\quad + g_2g_5(g_6 + \theta_B) - \alpha_V\psi(g_1 + g_2 + \theta_B) \\
&\quad - \left(\frac{\alpha_{VB}\psi\omega_1\Pi_V}{\theta_V K} + \frac{\alpha_{HB}\gamma\omega_2\Pi_H}{\theta_H K}\right), \\
m_4 &= g_1g_2g_5(g_6 + \theta_B) - g_6\theta_B(g_1g_2 + g_1g_5 + g_2g_5) \\
&\quad - \left(\frac{\alpha_{VB}\psi\omega_1\Pi_V(g_1 + g_2)}{\theta_V K} + \frac{\alpha_{HB}\gamma\omega_2\Pi_H(g_5 + g_6)}{\theta_H K}\right) \\
&\quad - \alpha_V\psi(g_1g_2 + \theta_Bg_1 + \theta_Bg_2), \\
m_5 &= g_1g_2g_5g_6\theta_B(1 - \mathcal{R}_0^L).
\end{aligned}$$

By applying the Routh–Hurwitz criterion Hassan et al. (2022), which states that all the roots of the polynomial (7) have negative real parts if and only if $m_1 > 0$, $m_2 > 0$, $m_3 > 0$, $m_4 > 0$, $m_5 > 0$, $m_1 m_2 m_3 > m_3^2 + m_1^2 m_4$, and $(m_1 m_4 - m_5)(m_1 m_2 m_3 - m_3^2 - m_1^2 m_4) > m_5 (m_1 m_2 - m_3)^2 + m_1 m_5^2$. Clearly, for all the conditions to be satisfied, then $\mathcal{R}_0^L < 1$. Thus, by Routh–Hurwitz criterion, the disease-free equilibrium of the Leptospirosis model (1) is locally asymptotically stable whenever $\mathcal{R}_0^L < 1$. □

3.4 Endemic equilibrium

In this section, we aim to explore the potential existence of an endemic equilibrium point, which represents a positive steady state where leptospirosis infection persists within the population. At this equilibrium point, the infected variables in the Leptospirosis model are non-zero (that is $E_H \neq 0$, $I_H \neq 0$, $T_H \neq 0$, $E_V \neq 0$, $I_V \neq 0$, and $B \neq 0$). To investigate this endemic equilibrium point, we solve the equations of the Leptospirosis model (1) in terms of the 'forces of infection,' expressed as:

$$\lambda_H^{**} = \frac{\alpha_H I_V^{**}}{N_H^{**}} + \frac{\alpha_{HB} B^{**}}{K + B^{**}}, \quad \textit{and} \quad \lambda_V^{**} = \frac{\alpha_V I_V^{**}}{N_V^{**}} + \frac{\alpha_{VB} B^{**}}{K + B^{**}} \tag{8}$$

With

$$\begin{aligned}
S_H^{**} &= \frac{\Pi_H g_1 g_2 g_3 g_4}{(\lambda_H^{**} + \theta_H) g_1 g_2 g_3 g_4 - \lambda_H^{*} \gamma \sigma \varepsilon \rho_H}, \\
E_H^{**} &= \frac{\lambda_H^{**} \Pi_H g_2 g_3 g_4}{(\lambda_H^{**} + \theta_H) g_1 g_2 g_3 g_4 - \lambda_H^{*} \gamma \sigma \varepsilon \rho_H}, \\
I_H^{**} &= \frac{\lambda_H^{**} \Pi_H \gamma g_3 g_4}{(\lambda_H^{**} + \theta_H) g_1 g_2 g_3 g_4 - \lambda_H^{*} \gamma \sigma \varepsilon \rho_H}, \\
T_H^{**} &= \frac{\lambda_H^{**} \Pi_H \gamma \sigma g_4}{(\lambda_H^{**} + \theta_H) g_1 g_2 g_3 g_4 - \lambda_H^{*} \gamma \sigma \varepsilon \rho_H}, \\
R_H^{**} &= \frac{\lambda_H^{**} \Pi_H \gamma \sigma \varepsilon}{(\lambda_H^{**} + \theta_H) g_1 g_2 g_3 g_4 - \lambda_H^{*} \gamma \sigma \varepsilon \rho_H}, \\
S_V^{**} &= \frac{\Pi_V g_5 g_6 g_7}{(\lambda_V^{**} + \theta_V) g_5 g_6 g_7 - \lambda_V^{**} \psi \tau \rho_V}, \\
E_V^{**} &= \frac{\lambda_V^{**} \Pi_V g_6 g_7}{(\lambda_V^{**} + \theta_V) g_5 g_6 g_7 - \lambda_V^{**} \psi \tau \rho_V}, \\
I_V^{**} &= \frac{\lambda_V^{**} \Pi_V \psi g_7}{(\lambda_V^{**} + \theta_V) g_5 g_6 g_7 - \lambda_V^{**} \psi \tau \rho_V}, \\
R_V^{**} &= \frac{\lambda_V^{**} \Pi_V \psi \tau}{(\lambda_V^{**} + \theta_V) g_5 g_6 g_7 - \lambda_V^{**} \psi \tau \rho_V}, \\
B^{**} &= \frac{\lambda_V^{**} \Pi_V \psi \omega_1 g_7}{\left((\lambda_V^{**} + \theta_V) g_5 g_6 g_7 - \lambda_V^{**} \psi \tau \rho_V\right) \theta_B} + \frac{\lambda_H^{**} \Pi_H \gamma \omega_2 g_3 g_4}{\left((\lambda_H^{**} + \theta_H) g_1 g_2 g_3 g_4 - \lambda_H^{*} \gamma \sigma \varepsilon \rho_H\right) \theta_B}.
\end{aligned} \tag{9}$$

Substituting (9) into (8), we obtained (38).

The structure of the polynomial (38) is suggestive of the phenomenon of backward bifurcation. This phenomenon is characterized by the coexistence of a stable disease-free equilibrium and a stable endemic equilibrium when the associated reproduction number of the Leptospirosis model is less than unity. In cases of backward bifurcation, there must be the existence of multiple endemic equilibria. Consequently, we examine the nature of the bifurcation in the following section.

3.5 Bifurcation analysis

In this section, we shall investigate the potential existence of a backward bifurcation by applying the Center Manifold Theorem, a concept thoroughly discussed by Castillo-Chavez and Song in their work (Castillo-Chavez and Song 2004).

Castillo-Chavez and Song theorem

Theorem 3 *Let us consider a general system of ordinary differential equations with a parameter* φ;

$$\frac{dx}{dt} = f(x, \varphi), f : \mathbb{R}^n \times \mathbb{R} \to \mathbb{R}^n, f \in \mathbf{C}^2(\mathbb{R}^n \times \mathbb{R}) \tag{10}$$

where $x = 0$ is an equilibrium point for the system in equation (10). That is, $f(0, \varphi) \equiv 0$ $\forall\ \varphi$.

Assume the following

H_1: $A = D_x f(0,0) = \left[\frac{\partial f}{\partial x}(0,0)\right]$ is the linearization matrix of the system given by equation (10) around the equilibrium 0 with φ evaluated at 0. Zero is a simple eigenvalue of A and other eigenvalues of A have negative real parts.

H_2: Matrix A has a non-negative right eigenvector w and a left eigenvector v corresponding to the zero eigenvalue.

Let f_k be the k^{th} component of f and

$$\begin{aligned} a &= \sum_{k,i,j=1}^{n} v_k w_i w_j \frac{\partial^2 f_k}{\partial x_i \partial x_j}(0,0), \\ b &= \sum_{k,i=1}^{n} v_k w_i \frac{\partial^2 f_k}{\partial x_i \partial \varphi}(0,0). \end{aligned} \tag{11}$$

The local dynamics of (10) around 0 are totally determined by the sign of a and b.

1. $a > 0, b > 0$; When $\varphi < 0$ with $|\varphi| << 1$, 0 is locally asymptotically stable and there exist a positive unstable equilibrium; when $0 < \varphi << 1$, 0 is unstable and there exist a negative, locally asymptotically stable equilibrium.
2. $a < 0, b < 0$; When $\varphi < 0$ with $|\varphi| << 1$, 0 is unstable; when $0 < \varphi << 1$, 0 is locally asymptotically stable equilibrium, and there exist a positive unstable equilibrium.
3. $a > 0, b < 0$; When $\varphi < 0$ with $|\varphi| << 1$, 0 is unstable, and there exist a locally asymptotically stable negative equilibrium; when $0 < \varphi << 1$, 0 is stable and a positive unstable equilibrium appears.

4. $a < 0$, $b > 0$; When φ changes from negative to positive, 0 changes its stability from stable to unstable. Correspondingly, a negative unstable equilibrium becomes positive and locally asymptotically stable.

In particular, if $a < 0$ and $b > 0$, then the bifurcation is forward; if $a > 0$ and $b > 0$, then the bifurcation is backward. Using this approach, the following result may be obtained.

Theorem 4 *The model of system* (1) *exhibits backward bifurcation at* $\mathcal{R}_0 = 1$.

Proof To apply the center manifold theorem, we will carry out some changes to the Lepstospirosis model (1) state variables. Let $S_H = x_1$, $E_H = x_2$, $I_H = x_3$, $T_H = x_4$, $R_H = x_5$, $S_V = x_6$, $E_V = x_7$, $I_V = x_8$, $R_V = x_9$, $B = x_{10}$. Using the vector notation $x = (x_1, x_2, x_3, \ldots, x_{10})^T$ and $\frac{dx}{dt} = F(x)$, with $F = (f_1, f_2, f_3, \ldots, f_{10})^T$. Hence the Leptospirosis model (1)becomes

$$
\begin{aligned}
\frac{dx_1}{dt} &\equiv f_1 = \Pi_H - \left(\frac{\alpha_H x_8}{x_1 + x_2 + x_3 + x_4 + x_5} + \frac{\alpha_{HB} x_{10}}{K + x_{10}}\right) x_1 - \theta_H x_1 + \rho_H x_5 \\
\frac{dx_2}{dt} &\equiv f_2 = \left(\frac{\alpha_H x_8}{x_1 + x_2 + x_3 + x_4 + x_5} + \frac{\alpha_{HB} x_{10}}{K + x_{10}}\right) x_1 - (\gamma + \theta_H) x_2 \\
\frac{dx_3}{dt} &\equiv f_3 = \gamma x_2 - (\sigma + \delta_H + \theta_H) x_3 \\
\frac{dx_4}{dt} &\equiv f_4 = \sigma x_3 - (\varepsilon + \phi\delta_H + \theta_H) x_4 \\
\frac{dx_5}{dt} &\equiv f_5 = \varepsilon x_4 - (\rho + \theta_H) x_5 \\
\frac{dx_6}{dt} &\equiv f_6 = \Pi_V - \left(\frac{\alpha_V x_8}{x_6 + x_7 + x_8 + x_9} + \frac{\alpha_{VB} x_{10}}{K + x_{10}}\right) x_6 - \theta_V x_6 + \rho_V x_9 \\
\frac{dx_7}{dt} &\equiv f_7 = \left(\frac{\alpha_V x_8}{x_6 + x_7 + x_8 + x_9} + \frac{\alpha_{VB} x_{10}}{K + x_{10}}\right) x_6 - (\psi + \theta_V) x_7 \\
\frac{dx_8}{dt} &\equiv f_8 = \psi x_7 - (\tau + \delta_V + \theta_V) x_8 \\
\frac{dx_9}{dt} &\equiv f_9 = \tau x_8 - (\rho_V + \theta_V) x_9 \\
\frac{dx_{10}}{dt} &\equiv f_{10} = \omega_1 x_8 + \omega_2 x_3 - \theta_B x_{10},
\end{aligned}
\tag{12}
$$

Considering $\alpha_{HB} = \alpha^*_{HB}$, as the bifurcation parameter at $\mathcal{R}^L_0 = 1$, we have

$$
\alpha^*_{HB} = \frac{\theta_B \theta_H \theta_V K g_1 g_2 (g_5 g_6 - \alpha_V \psi) - \alpha_{VB} \Pi_V \psi \theta_H (\omega_1 g_1 g_2 + \alpha_H \gamma \omega_2)}{\Pi_H \gamma \omega_2 \theta_V (g_5 g_6 - \alpha_V \psi)}
$$

Computing the Jacobian of the transformed system (12) at the Disease-Free Equilibrium (DFE), denoted as (ξ_0) with $\alpha_{HB} = \alpha^*_{HB}$, yields:

$$J(\xi_0)|_{\alpha_{HB}=\alpha^*_{HB}} = \begin{bmatrix} -\theta_H & 0 & 0 & 0 & \rho_H & 0 & 0 & -\alpha_H & 0 & -\frac{\alpha^*_{HB}\Pi_H}{\theta_H K} \\ 0 & -g_1 & 0 & 0 & 0 & 0 & 0 & \alpha_H & 0 & \frac{\alpha^*_{HB}\Pi_H}{\theta_H K} \\ 0 & \gamma & -g_2 & 0 & 0 & 0 & 0 & 0 & 0 & 0 \\ 0 & 0 & \sigma & -g_3 & 0 & 0 & 0 & 0 & 0 & 0 \\ 0 & 0 & 0 & \varepsilon & -g_4 & 0 & 0 & 0 & 0 & 0 \\ 0 & 0 & 0 & 0 & 0 & -\theta_V & 0 & -\alpha_V & \rho_V & -\frac{\alpha_{VB}\Pi_V}{\theta_V K} \\ 0 & 0 & 0 & 0 & 0 & 0 & -g_5 & \alpha_V & 0 & \frac{\alpha_{VB}\Pi_V}{\theta_V K} \\ 0 & 0 & 0 & 0 & 0 & 0 & \psi & -g_6 & 0 & 0 \\ 0 & 0 & 0 & 0 & 0 & 0 & 0 & \tau & -g_7 & 0 \\ 0 & 0 & \omega_2 & 0 & 0 & 0 & 0 & \omega_1 & 0 & -\theta_B \end{bmatrix}$$

where

$g_1 = \gamma + \theta_H$, $g_2 = \sigma + \delta_H + \theta_H$, $g_3 = \varepsilon + \phi\delta_H + \theta_H$, $g_4 = \rho_H + \theta_H$, $g_5 = \psi + \theta_V$, $g_6 = \tau + \delta_V + \theta_V$, and $g_7 = \rho_V + \theta_V$.

The right eigenvector, denoted as $w = (w_1, w_2, w_3, w_4, w_5, w_6, w_7, w_8, w_9, w_{10})^T$, corresponding to the simple zero eigenvalue, can be derived from $J(\xi_0)|_{\alpha_{HB}=\alpha^*_{HB}} w = 0$, given by

$$\begin{aligned}
&-\theta_H w_1 + \rho w_5 - \alpha_H w_8 - \frac{\alpha^*_{HB}\Pi_H w_{10}}{\theta_H K} = 0 \\
&-g_1 w_2 + \alpha_H w_8 + \frac{\alpha^*_{HB}\Pi_H w_{10}}{\theta_H K} = 0 \\
&\gamma w_2 - g_2 w_3 = 0 \\
&\sigma w_3 - g_3 w_4 = 0 \\
&\varepsilon w_4 - g_4 w_5 = 0 \\
&-\theta_V w_6 - \alpha_V w_8 + \rho_V w_9 - \frac{\alpha_{VB}\Pi_V w_{10}}{\theta_V K} = 0 \\
&-g_5 w_7 + \alpha_V w_8 + \frac{\alpha_{VB}\Pi_V w_{10}}{\theta_V K} = 0 \\
&\psi w_7 - g_6 w_8 = 0 \\
&\tau w_8 - g_7 w_9 = 0 \\
&\omega_2 w_3 + \omega_1 w_8 - \theta_B w_{10} = 0
\end{aligned} \tag{13}$$

From the equation (13), we obtained

$$
\begin{aligned}
w_1 &= \frac{\left(\rho_H\varepsilon\sigma\theta_B - \alpha^*_{HB}\Pi_H\omega_2 g_3 g_4\right)w_3}{\theta_B\theta_H g_3 g_4} - \frac{\left(\alpha_H\theta_B + \alpha^*_{HB}\Pi_H\omega_1\right)w_8}{\theta_B\theta_H},\\
w_2 &= \frac{g_2 w_3}{\gamma}, w_3 = w_3 > 0, w_4 = \frac{\sigma w_3}{g_3},\\
w_5 &= \frac{\varepsilon\sigma w_3}{g_3 g_4}, w_6 = \frac{\left(\tau\psi\rho_V - g_5 g_6 g_7\right)w_8}{\psi g_7}, w_7 = \frac{g_6 w_8}{\psi},\\
w_8 &= w_8 > 0, w_9 = \frac{\tau w_8}{g_7}, and \quad w_{10} = \frac{\omega_2 w_3 + \omega_1 w_8}{\theta_B}.
\end{aligned}
\tag{14}
$$

Likewise, the left eigenvector, denoted as $v = \left(v_1, v_2, v_3, v_4, v_5, v_6, v_7, v_8, v_9, v_{10}\right)$, satisfying $v.w = 1$, associated with the simple zero eigenvalue, can be determined from $vJ\left(\xi_0\right)|_{\alpha_{HB}=\alpha^*_{HB}} = 0$, given by

$$
\begin{aligned}
-\theta_H v_1 &= 0\\
-g_1 v_2 + \gamma v_3 &= 0\\
-g_2 v_3 + \sigma v_4 + \omega_2 v_{10} &= 0\\
-g_3 v_4 + \varepsilon v_5 &= 0\\
\rho v_1 + g_4 v_5 &= 0\\
-\theta_V v_6 &= 0\\
-g_5 v_7 + \psi v_8 &= 0\\
-\alpha_H v_1 + \alpha_H v_2 - \alpha_V v_6 + \alpha_V v_7 - g_6 v_8 + \tau v_9 + \omega_1 v_{10} &= 0\\
-\rho_V v_6 - g_7 v_9 &= 0\\
-\frac{\alpha^*_{HB}\Pi_H v_1}{\theta_H K} + \frac{\alpha^*_{HB}\Pi_H v_2}{\theta_H K} - \frac{\alpha_{VB}\Pi_V v_6}{\theta_V K} + \frac{\alpha_{VB}\Pi_V v_7}{\theta_V K} - \theta_B v_{10} &= 0
\end{aligned}
\tag{15}
$$

From (15) above, we obtained

$$
\begin{aligned}
v_1 = v_4 = v_5 = v_6 = v_9 = 0, v_2 = v_2 > 0, v_3 = \frac{g_1 v_2}{\gamma}, v_7 = v_7 > 0,\\
v_8 = \frac{g_5 v_7}{\psi}, v_{10} = \frac{\alpha^*_{HB}\Pi_H v_2}{\theta_H\theta_B K} + \frac{\alpha_{VB}\Pi_V v_7}{\theta_V\theta_B K}.
\end{aligned}
\tag{16}
$$

Computation of a and b

Since $v_1 = v_4 = v_5 = v_6 = v_9 = 0$ for $k = 1, 2, 3, \ldots, 10$, the only non-zero partial derivatives are

$$
\begin{aligned}
&\frac{\partial^2 f_2}{\partial x_2\partial x_8} = \frac{\partial^2 f_2}{\partial x_8\partial x_2} = \frac{\partial^2 f_2}{\partial x_3\partial x_8} = \frac{\partial^2 f_2}{\partial x_8\partial x_3} = \frac{\partial^2 f_2}{\partial x_4\partial x_8} = \frac{\partial^2 f_2}{\partial x_8\partial x_4} = \frac{\partial^2 f_2}{\partial x_5\partial x_8} = \frac{\partial^2 f_2}{\partial x_8\partial x_5} = -\frac{\alpha_H\theta_H}{\Pi_H},\\
&\frac{\partial^2 f_2}{\partial x_1\partial x_{10}} = \frac{\partial^2 f_2}{\partial x_{10}\partial x_1} = \frac{\alpha_{HB}}{K}, \frac{\partial^2 f_2}{\partial x_{10}^2} = -\frac{2\alpha_{HB}\Pi_H}{\theta_H K^2}, \frac{\partial^2 f_7}{\partial x_6\partial x_{10}} = \frac{\partial^2 f_7}{\partial x_{10}\partial x_6} = \frac{\alpha_{VB}}{K}, \frac{\partial^2 f_7}{\partial x_{10}^2} = -\frac{2\alpha_{VB}\Pi_V}{\theta_V K^2},\\
&\frac{\partial^2 f_7}{\partial x_7\partial x_8} = \frac{\partial^2 f_7}{\partial x_8\partial x_7} = \frac{\partial^2 f_7}{\partial x_8\partial x_9} = \frac{\partial^2 f_7}{\partial x_9\partial x_8} = -\frac{\alpha_V\theta_V}{\Pi_V}, \frac{\partial^2 f_7}{\partial x_8^2} = -\frac{2\alpha_V\theta_V}{\Pi_V}, \frac{\partial^2 f_2}{\partial x_{10}\partial\alpha^*_{HB}} = \frac{\Pi_H}{\theta_H K}.
\end{aligned}
\tag{17}
$$

But

$$a = \sum_{k,i,j=1}^{n} v_k w_i w_j \frac{\partial^2 f_k}{\partial x_i \partial x_j}(\xi_0)$$

$$a = -\frac{2v_2 w_3 w_8 \alpha_H \theta_H \left(g_2 g_3 g_4 + \gamma g_3 g_4 + \sigma\gamma g_4 + \varepsilon\sigma\gamma\right)}{\Pi_H \gamma g_3 g_4} - \frac{2v_2\left(\omega_2 w_3 + \omega_1 w_8\right)^2 \alpha^*_{HB} \Pi_H}{\theta_B^2 \theta_H K^2} + \frac{2v_2\left(\omega_2 w_3 + \omega_1 w_8\right)\alpha^*_{HB}}{\theta_B K}\left(\frac{\left(\rho_H \varepsilon\sigma\theta_B - \alpha^*_{HB}\Pi_H \omega_2 g_3 g_4\right) w_3}{\theta_B \theta_H g_3 g_4} - \frac{\left(\alpha_H \theta_B + \alpha^*_{HB}\Pi_H \omega_1\right) w_8}{\theta_B \theta_H}\right) + \frac{2v_7 w_8\left(\omega_2 w_3 + \omega_1 w_8\right)\left(\tau\psi\rho_V - g_5 g_6 g_7\right)\alpha_{VB}}{\theta_B \psi K g_7} - \frac{2v_7\left(\omega_2 w_3 + \omega_1 w_8\right)^2 \alpha_{VB}\Pi_V}{\theta_B^2 \theta_V K^2} - \frac{2v_7 w_8^2 \alpha_V \theta_V}{\Pi_V} - \frac{2v_7 w_8^2 \alpha_V \theta_V \left(g_6 g_7 + \tau\psi\right)}{\Pi_V \psi g_7} < 0. \tag{18}$$

and

$$b = \sum_{k,i=1}^{n} v_k w_i \frac{\partial^2 f_k}{\partial x_i \partial \alpha^*_d}(\xi_0)$$

$$b = \frac{v_2\left(\omega_2 w_3 + \omega_1 w_8\right)\Pi_H}{\theta_B \theta_H K} > 0. \tag{19}$$

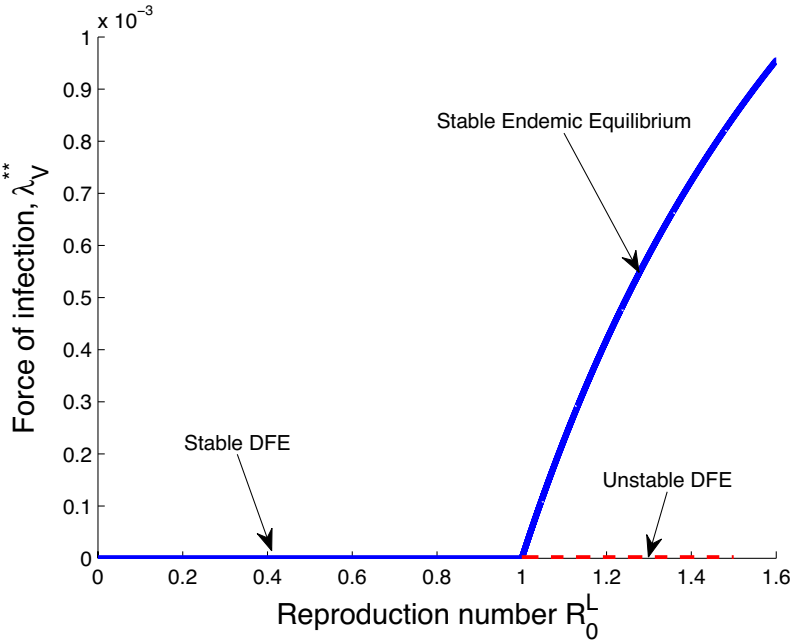

Fig. 2 Forward bifurcation of the Leptospirosis model

Consequently, given that the bifurcation coefficient b is positive and the sign of the coefficient of a is negative, according to theorem 5 in Castillo-Chavez and Song (2004), it can be concluded that the Leptospirosis model undergoes a forward bifurcation at $\mathcal{R}_0^L = 1$ whenever $a < 0$. Thus, the endemic equilibrium has a unique positive equilibrium and it is locally asymptotically stable for $\mathcal{R}_0^L > 1$. Figure 2, Illustrate forward bifurcation of the Leptospirosis model. □

Biologically, this outcome implies that the leptospirosis disease has the potential for eradication from the population when the Leptospirosis reproduction number, denoted as $\mathcal{R}_0^L$, is less than one ($\mathcal{R}_0^L < 1$). □

3.6 Global stability of the disease-free equilibrium

The Leptospirosis model (1) can be written as

$$\begin{aligned} \frac{dX}{dt} &= F(X, Y) \\ \frac{dY}{dt} &= G(X, Y) \qquad F(X, 0) = 0 \end{aligned} \tag{20}$$

Where $X = \left(S_H, R_H, S_V, R_V\right)$ and $Y = \left(E_H, I_H, T_H, E_V, I_V, B\right)$ with $X \in \mathfrak{R}_+^4$ denoting the number of uninfected compartments and $Z \in \mathfrak{R}_+^6$ denoting the number of infected compartments. Let $\xi_0 = (X^*, 0)$ represents the disease-free equilibrium point of the system (1).

ξ_0 is globally asymptotically stable equilibrium for the Leptospirosis model (1) if it satisfies condition $\mathscr{A}_1$ and $\mathscr{A}_2$ below

$\mathscr{A}_1$: $\frac{dX}{dt} = F(X, 0)$, X^* is globally asymptotically stable.

$\mathscr{A}_2$: $\frac{dY}{dt} = D_Y G(X^*, 0)Y - \hat{G}(X, Y)$, $\hat{G}(X, Y) \geq 0$ for all $(X, Y) \in \mathcal{D}$.

Where $D_Y G(X^*, 0)$ is the Jacobian of $G(X, Y)$ taking in $\left(E_H, I_H, T_H, E_V, I_V, B\right)$ and evaluated at $(X^*, 0) = \left(\left(\frac{\Pi_H}{\theta_H}, 0, \frac{\Pi_V}{\theta_V}, 0\right), 0\right)$. If the system (20) satisfies the conditions, then the following theorem holds.

Theorem 5 *The equilibrium point* $(X^*, 0)$ *of the system* (20) *is globally asymptotically stable if* $\mathcal{R}_0^L \leq 1$, *and condition* $\mathscr{A}_1$ *and* $\mathscr{A}_2$ *are satisfied.*

Proof From the system (1) we obtain $F(X, Y)$ and $G(X, Y)$ as

$$F(X,Y)=\begin{bmatrix}\Pi_H-\left(\frac{\alpha_H I_V}{N_H}+\frac{\alpha_{HB}B}{K+B}\right)S_H-\theta_H S_H+\rho_H R_H\\ \varepsilon T_H-\left(\rho_H+\theta_H\right)R_H\\ \Pi_V-\left(\frac{\alpha_V I_V}{N_V}+\frac{\alpha_{VB}B}{K+B}\right)S_V-\theta_V S_V+\rho_V R_V\\ \tau I_V-\left(\rho_V+\theta_V\right)R_V\end{bmatrix}$$

$$G(X,Y)=\begin{bmatrix}\left(\frac{\alpha_H I_V}{N_H}+\frac{\alpha_{HB}B}{K+B}\right)S_H-\left(\gamma+\theta_H\right)E_H\\ \gamma E_H-\left(\sigma+\delta_H+\theta_H\right)I_H\\ \sigma I_H-\left(\varepsilon+\phi\delta_H+\theta_H\right)T_H\\ \left(\frac{\alpha_V I_V}{N_V}+\frac{\alpha_{VB}B}{K+B}\right)S_V-\left(\psi+\theta_V\right)E_V\\ \psi E_V-\left(\tau+\delta_V+\theta_V\right)I_V\\ \omega_1 I_V+\omega_2 I_H-\theta_B B\end{bmatrix}$$

Now, we consider $\frac{dX}{dt}=F(X,0)$ the reduced system from condition $\mathscr{A}_1$

$$\begin{aligned}\frac{dS_H}{dt}&=\Pi_H-\theta_H S_H\\ \frac{dR_H}{dt}&=0\\ \frac{dS_V}{dt}&=\Pi_V-\theta_V S_V\\ \frac{dR_V}{dt}&=0\end{aligned}\tag{21}$$

$X^*=\left(\frac{\Pi_H}{\theta_H},0,\frac{\Pi_V}{\theta_V},0\right)$ is a globally asymptotically stable equilibrium point for the reduced system $\frac{dX}{dt}=F(X,0)$ in (21). We note that this asymptotic dynamics is independent of the initial condition in $\mathcal{D}$. Therefore, the convergence of the solution of the reduced system (21) is global in $\mathcal{D}$. Hence, we compute

$$D_Y G(X^*,0)=\begin{bmatrix}-\left(\gamma+\theta_H\right) & 0 & 0 & 0 & \alpha_H & \frac{\alpha_{HB}\Pi_H}{\theta_H K}\\ \gamma & -\left(\sigma+\delta_H+\theta_H\right) & 0 & 0 & 0 & 0\\ 0 & \sigma & -\left(\varepsilon+\phi\delta_H+\theta_H\right) & 0 & 0 & 0\\ 0 & 0 & 0 & -\left(\psi+\theta_V\right) & \alpha_V & \frac{\alpha_{VB}\Pi_V}{\theta_V K}\\ 0 & 0 & 0 & \psi & -\left(\tau+\delta_V+\theta_V\right) & 0\\ 0 & \omega_2 & 0 & 0 & \omega_1 & -\theta_B\end{bmatrix}$$

$$\hat{G}(X,Y)=\begin{bmatrix}\alpha_H I_H\left(1-\frac{S_H}{N_H}\right)+\alpha_{HB}B\left(\frac{\Pi_H}{\theta_H K}-\frac{S_H}{K+B}\right)\\ 0\\ 0\\ \alpha_V I_V\left(1-\frac{S_V}{N_V}\right)+\alpha_{VB}B\left(\frac{\Pi_V}{\theta_V K}-\frac{S_V}{K+B}\right)\\ 0\\ 0\end{bmatrix}$$

Thus, since $S_H\le N_H\le\frac{\Pi_H}{\theta_H}$, and $S_V\le N_V\le\frac{\Pi_V}{\theta_V}$, then $\hat{G}(X,Y)\ge 0$ for all $(X,Y)\in\mathcal{D}$. Therefore, this prove that the disease-free equilibrium is globally asymptotically stable when $\mathcal{R}_0^L\le 1$. □

3.7 Data-fitting and parameter estimation

In this section, we Fitted the Leptospirosis model to the confirmed cases of leptospirosis in Kerala State, India, covering the period from January 2021 to December 2022. The data on confirmed leptospirosis cases were obtained from the State Surveillance Unit, Directorate of Health, Government of Kerala (Directorate of Health Services), as outlined in Table 2. The data fitting was conducted using MATLAB and the fmincon function in the Optimization Toolbox (McCall 2005). This method employs the least squares approach, known for its efficiency and reliability. The goal is to align the observed data set, Y_i, with the estimated values, X_i, aiming to minimize the sum of squares errors (SSE), expressed mathematically as:

$$SSE = \sum_{i=1}^{k} (Y_i - X_i)^2 \tag{22}$$

We estimated the population of Kerala State to be 34,840,000 (Population Census), and the initial values of the state variables used for the data-fitting are $S_H(0) = 33837925$, $E_H(0) = 1000000$, $I_H(0) = 2000$, $T_H(0) = 75$, $R_H(0) = 0$, $S_V(0) = 15000$, $E_V(0) = 1000$, $I_V(0) = 200$, $R_V(0) = 0$, and $B(0) = 500$. The fitting results are illustrated in Fig. 3.

Table 2 Kerela State Data for the monthly confirmed cases of Leptospirosis from January, 2021 to December, 2022

Month	Case	Death
Jan 2021	75	3
Feb 2021	111	3
Mar 2021	57	2
Apr 2021	42	2
May 2021	40	3
Jun 2021	132	12
Jul 2021	152	5
Aug 2021	181	8
Sep 2021	179	13
Oct 2021	210	17
Nov 2021	285	10
Dec 2021	281	19
Jan 2022	107	2
Feb 2022	109	3
Mar 2022	123	8
Apr 2022	123	2
May 2022	167	5
Jun 2022	235	13
Jul 2022	305	21
Aug 2022	377	21
Sep 2022	274	7
Oct 2022	233	12
Nov 2022	226	10
Dec 2022	203	17

Table 3 Parameter values for model (1)

Parameter	Value	Source
Π_H	0.0132	CEIC data
Π_V	1.2	El-Shahed (2014)
α_H	0.0828	Fitted
α_V	0.01	Fitted
α_{HB}	3.0835×10^{-6}	Fitted
α_{VB}	0.0170	Fitted
θ_H	0.007	Urban death rates in India (2020)
θ_V	0.003	Alemneh (2020)
θ_B	0.05	Minter et al. (2019)
γ	0.092	Khan et al. (2012)
σ	0.001	Fitted
δ_H	0.0004	Fitted
δ_V	0.0018	Alemneh (2020)
ϕ	0.001	Fitted
ε	0.0027	Alemneh (2020)
τ	0.0519	Fitted
ρ_H	0.089	Khan et al. (2014)
ρ_V	0.001	Fitted
ψ	0.6090	Fitted
ω_1	0.02	Fitted
ω_2	0.006	Fitted
K	10,000	Engida et al. (2022)

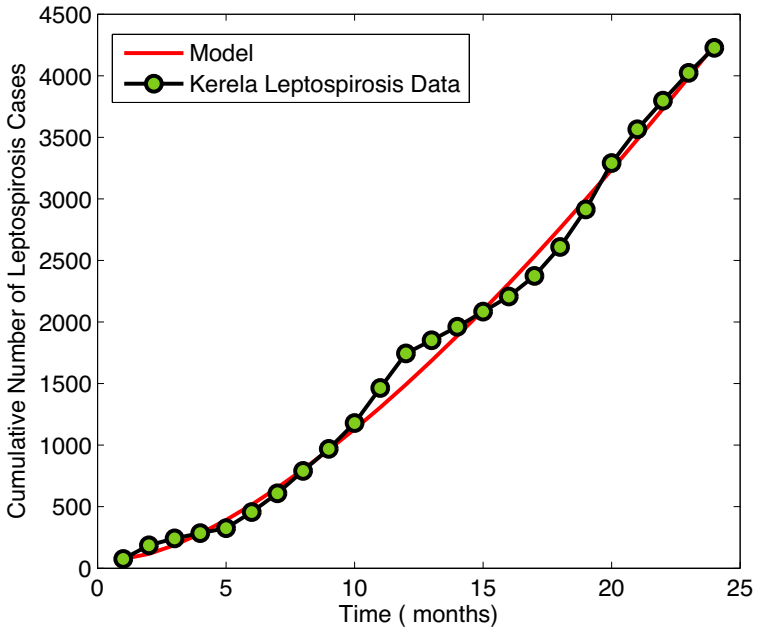

Fig. 3 Cumulative Number of Leptospirosis Cases in Kerela from January, 2021 to December, 2022

3.8 Sensitivity analysis

In this section, our focus is on conducting a sensitivity analysis for the fundamental parameters contributing to the basic reproduction number of the Leptospirosis model (1). The objective is to assess the importance of each parameter in influencing the transmission dynamics of Leptospirosis. To achieve this, we adopt the methodology outlined in Oguntolu et al. (2023); Omede et al. (2023). Following the principles articulated in Oguntolu et al. (2023); Omede et al. (2023), we leverage the normalized forward sensitivity index of a variable denoted as 'Z', which exhibits differential dependence on the parameter 'p', defined as

$$\mathscr{G}_p^Z = \frac{\partial Z}{\partial p} \times \frac{p}{Z}. \tag{23}$$

Thus, the sensitivity index of the basic reproduction number of Leptospirosis model (1) with respect to the parameter 'p', can be computed as

$$\mathscr{G}_p^{\mathcal{R}_0^L} = \frac{\partial \mathcal{R}_0^L}{\partial p} \times \frac{p}{\mathcal{R}_0^L}. \tag{24}$$

Therefore, the sensitive indices of the basic reproduction number with respect to the basic parameters is computed as follows;

$$\mathscr{G}_{\alpha_V}^{\mathcal{R}_0^L} = \left(\frac{\psi}{(\psi+\theta_V)(\tau+\delta_V+\theta_V)} - \frac{\Pi_H \alpha_{HB} \gamma \psi \omega_2}{\theta_H \theta_B K (\gamma+\theta_H)(\sigma+\delta_H+\theta_H)(\psi+\theta_V)(\tau+\delta_V+\theta_V)} \right) \times \frac{\alpha_V \theta_H \theta_V \theta_B K g_1 g_2 g_5 g_6}{\alpha_V \psi \theta_H \theta_V \theta_B K g_1 g_2 + \alpha_{VB} \psi \omega_1 \Pi_V \theta_H g_1 g_2 + \alpha_{HB} \gamma \omega_2 \Pi_H \theta_V g_5 g_6 + (\alpha_{VB} \alpha_H \Pi_V \theta_H - \alpha_{HB} \alpha_V \Pi_H \theta_V) \gamma \psi \omega_2},$$

where

$g_1 = \gamma + \theta_H$, $g_2 = \sigma + \delta_H + \theta_H$, $g_3 = \varepsilon + \phi\delta_H + \theta_H$, $g_4 = \rho + \theta_H$, $g_5 = \psi + \theta_V$, and $g_6 = \tau + \delta_V + \theta_V$.

We have that

$$\mathscr{G}_{\alpha_V}^{\mathcal{R}_0^L} = 0.9075,$$

$$\mathscr{G}_{\alpha_H}^{\mathcal{R}_0^L} = \frac{\Pi_V \alpha_{VB} \gamma \psi \omega_2}{\theta_V \theta_B K (\gamma+\theta_H)(\sigma+\delta_H+\theta_H)(\psi+\theta_V)(\tau+\delta_V+\theta_V)} \times \frac{\alpha_H \theta_H \theta_V \theta_B K g_1 g_2 g_5 g_6}{\alpha_V \psi \theta_H \theta_V \theta_B K g_1 g_2 + \alpha_{VB} \psi \omega_1 \Pi_V \theta_H g_1 g_2 + \alpha_{HB} \gamma \omega_2 \Pi_H \theta_V g_5 g_6 + (\alpha_{VB} \alpha_H \Pi_V \theta_H - \alpha_{HB} \alpha_V \Pi_H \theta_V) \gamma \psi \omega_2}$$

We have that

$$\mathscr{G}_{\alpha_H}^{\mathcal{R}_0^L} = 0.0678.$$

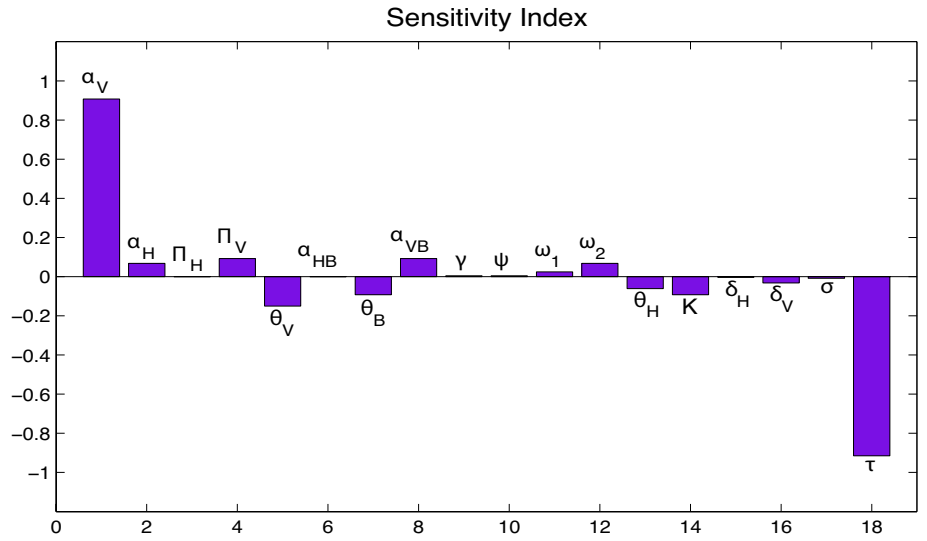

Fig. 4 Sensitivity index of the basic reproduction number of the Leptospirosis model

In similar reasoning, we obtained the sensitivity indices of the remaining basic parameters that constitute the basic reproduction number, and is given by

$$\begin{aligned}
&\mathscr{G}^{\mathcal{R}_0^L}_{\alpha_{HB}} = 3.291 \times 10^{-8}, \mathscr{G}^{\mathcal{R}_0^L}_{\alpha_{VB}} = 0.0925, \mathscr{G}^{\mathcal{R}_0^L}_{\gamma} = 0.0048, \mathscr{G}^{\mathcal{R}_0^L}_{\psi} = 0.0049,\\
&\mathscr{G}^{\mathcal{R}_0^L}_{\omega_1} = 0.0247, \mathscr{G}^{\mathcal{R}_0^L}_{\omega_2} = 0.0678, \mathscr{G}^{\mathcal{R}_0^L}_{\Pi_V} = 0.0925, \mathscr{G}^{\mathcal{R}_0^L}_{\Pi_H} = 3.291 \times 10^{-8},\\
&\mathscr{G}^{\mathcal{R}_0^L}_{\theta_B} = -0.0925, \mathscr{G}^{\mathcal{R}_0^L}_{\theta_H} = -0.0613, \mathscr{G}^{\mathcal{R}_0^L}_{\theta_V} = -0.1503, \mathscr{G}^{\mathcal{R}_0^L}_{K} = -0.0925,\\
&\mathscr{G}^{\mathcal{R}_0^L}_{\delta_H} = -0.0032, \mathscr{G}^{\mathcal{R}_0^L}_{\delta_V} = -0.0317, \mathscr{G}^{\mathcal{R}_0^L}_{\tau} = -0.9153, \mathscr{G}^{\mathcal{R}_0^L}_{\sigma} = -0.0081.
\end{aligned}$$

3.8.1 Interpretation of the sensitivity indices

The bar chart in Fig. 4 illustrates the sensitivity indices of the basic reproduction number for the Leptospirosis model. Parameters displaying positive indices exert a substantial influence on expediting the disease spread. Specifically, as the values of these parameters increase, while keeping other parameters constant, there is a notable escalation in the basic reproduction number. Consequently, an augmentation in the values of these parameters contributes to an increase in the overall disease transmission. Conversely, parameters characterized by negative indices play a pivotal role in alleviating disease burdens. When these parameters experience an increase in values, there is a corresponding reduction in the basic reproduction number, indicating a mitigated impact on the spread of the disease.

4 Optimal control

Building on the findings of the sensitivity analysis, we introduced three time-dependent control measures, denoted as $u_1(t)$, $u_2(t)$, and $u_3(t)$, aimed at mitigating the spread of leptospirosis. These measures encapsulate preventive actions, such as the utilization of hand gloves and goggles during animal handling, wearing of rubber boots in times of flooding or heavy rainfall (represented by $u_1(t)$), animal vaccination ($u_2(t)$), and environmental sanitation practices, which involve the clearance of drainages and removal of trash from the surroundings ($u_3(t)$). Therefore, the Leptospirosis model with the time dependent control measures becomes

$$\begin{aligned}
\frac{dS_H}{dt} &= \Pi_H - \big(1-u_1(t)\big)\left(\frac{\alpha_H I_V}{N_H} + \frac{\alpha_{HB} B}{K+B}\right)S_H - \theta_H S_H + \rho_H R_H \\
\frac{dE_H}{dt} &= \big(1-u_1(t)\big)\left(\frac{\alpha_H I_V}{N_H} + \frac{\alpha_{HB} B}{K+B}\right)S_H - \big(\gamma+\theta_H\big)E_H \\
\frac{dI_H}{dt} &= \gamma E_H - \big(\sigma+\delta_H+\theta_H\big)I_H \\
\frac{dT_H}{dt} &= \sigma I_H - \big(\varepsilon+\phi\delta_H+\theta_H\big)T_H \\
\frac{dR_H}{dt} &= \varepsilon T_H - \big(\rho_H+\theta_H\big)R_H \\
\frac{dS_V}{dt} &= \Pi_V - \left(\frac{\alpha_V I_V}{N_V} + \frac{\alpha_{VB} B}{K+B}\right)S_V - \big(u_2(t)+\theta_V\big)S_V + \rho_V R_V \\
\frac{dE_V}{dt} &= \left(\frac{\alpha_V I_V}{N_V} + \frac{\alpha_{VB} B}{K+B}\right)S_V - \big(\psi+\theta_V\big)E_V \\
\frac{dI_V}{dt} &= \psi E_V - \big(\tau+\delta_V+\theta_V+u_2(t)\big)I_V \\
\frac{dR_V}{dt} &= \tau I_V + u_2(t)\big(S_V+I_V\big) - \big(\rho_V+\theta_V\big)R_V \\
\frac{dB}{dt} &= \omega_1 I_V + \omega_2 I_H - \big(u_3(t)+\theta_B\big)B
\end{aligned} \tag{25}$$

For this, we establish the objective functional as follows;

$$J(u) = \int_0^{t_f} \left[a_1 I_H + a_2\big(S_V + E_V + I_V + R_V\big) + a_3 B + \frac{1}{2}\sum_{i=1}^{3} b_i u_i^2(t)\right] dt \tag{26}$$

Here, the parameter a_i, $(i = 1, 2, 3)$ and b_i, $(i = 1, 2, 3)$ are the weight factors to help balance each terms in the integrand in (26), so that none of the terms dominate. The terms in the integrand in (26) are explained as follows;

1. The term $a_1 I_H + a_2\big(S_V + E_V + I_V + R_V\big) + a_3 B$, denotes the expenses in monitoring infected individuals and the animal population at all stages.
2. The term $b_1 u_1^2(t) + b_3 u_3^2(t)$, represents the cost associated with the public health awareness campaign to educate the public on sanitation and ways to prevent susceptible individuals from acquiring leptospirosis.
3. The term $b_2 u_2^2(t)$, represents the cost associated with the vaccination of animals.

The objective is to minimize the total count of individuals and animals within specified infectious classes, while simultaneously minimizing the costs associated with the implemented controls ($u_1(t)$, $u_2(t)$, and $u_3(t)$). The goal is to find an optimal control ($u_1^*(t)$, $u_2^*(t)$, and $u_3^*(t)$) such that

$$J\left[u_1^*, u_2^*, u_3^*\right] = \min_{u_i \in \Omega} J\left[u_1, u_2, u_3\right] \tag{27}$$

Where

$$\Omega = \left\{\left(u_1^*(t), u_2^*(t), u_3^*(t)\right) \in \mathscr{L}\left(0, t_f\right) \times \mathscr{L}\left(0, t_f\right) | a_i \leq u_i \leq b_i, i = 1, 2, 3\right\} \tag{28}$$

is lesbgue measurable.

4.1 Characterization of the optimal controls

The necessary conditions that an optimal control must satisfy comes from the Pontryagin's Maximum Principle (Pontryagin 2018). This principle converts equation (25) and (26) into a problem of minimizing pointwise a Hamiltonian $\mathcal{H}$, with respect to the controls $(u_1(t), u_2(t), u_3(t))$. First we formulate the Hamiltonian from the objective functional (26) and the governing dynamics (25) to obtain the optimality conditions, given by

$$\begin{aligned}
\mathcal{H} = {} & a_1 I_H + a_2\left(S_V + E_V + I_V + R_V\right) + a_3 B + \frac{1}{2}\sum_{i=1}^{3} b_i u_i^2(t) + \\
& \lambda_1\left[\Pi_H - \left(1 - u_1(t)\right)\left(\frac{\alpha_H I_V}{N_H} + \frac{\alpha_{HB} B}{K + B}\right)S_H - \theta_H S_H + \rho_H R_H\right] + \\
& \lambda_2\left[\left(1 - u_1(t)\right)\left(\frac{\alpha_H I_V}{N_H} + \frac{\alpha_{HB} B}{K + B}\right)S_H - \left(\gamma + \theta_H\right)E_H\right] + \lambda_3\left[\gamma E_H - \left(\sigma + \delta_H + \theta_H\right)I_H\right] + \\
& \lambda_4\left[\sigma I_H - \left(\varepsilon + \phi\delta_H + \theta_H\right)T_H\right] + \lambda_5\left[\varepsilon T_H - \left(\rho_H + \theta_H\right)R_H\right] + \\
& \lambda_6\left[\Pi_V - \left(\frac{\alpha_V I_V}{N_V} + \frac{\alpha_{VB} B}{K + B}\right)S_V - \left(u_2(t) + \theta_V\right)S_V + \rho_V R_V\right] + \\
& \lambda_7\left[\left(\frac{\alpha_V I_V}{N_V} + \frac{\alpha_{VB} B}{K + B}\right)S_V - \left(\psi + \theta_V\right)E_V\right] + \lambda_8\left[\psi E_V - \left(\tau + \delta_V + \theta_V + u_2(t)\right)I_V\right] + \\
& \lambda_9\left[\tau I_V + u_2(t)\left(S_V + I_V\right) - \left(\rho_V + \theta_V\right)R_V\right] + \lambda_{10}\left[\omega_1 I_V + \omega_2 I_H - \left(u_3(t) + \theta_B\right)B\right].
\end{aligned} \tag{29}$$

Where $\lambda_1, \lambda_2, \lambda_3, \lambda_4, \lambda_5, \lambda_6, \lambda_7, \lambda_8, \lambda_9, \lambda_{10}$ are the adjoint functions associated to the state variables $S_H, E_H, I_H, T_H, R_H, S_V, E_V, I_V, R_V, B$. The system of adjoint equations is obtained by taking the partial derivatives of the Hamiltonian (29) with respect to the associated state and control variables.

Theorem 6 *Given the optimal control sets u_1^*, u_2^*, u_3^* and the solutions S_H^*, E_H^*, I_H^*, T_H^*, R_H^*, S_V^*, E_V^*, I_V^*, R_V^*, B^* of the corresponding state system (25) that minimizes $J(u_1, u_2, u_3)$ over Ω, then there exists adjoint functions $\lambda_1, \lambda_2, \lambda_3, \lambda_4, \lambda_5, \lambda_6, \lambda_7, \lambda_8, \lambda_9, \lambda_{10}$, such that*

$$
\begin{aligned}
\frac{d\lambda_1}{dt} &= \frac{(1-u_1)\alpha_H I_V S_H(\lambda_2-\lambda_1)}{N_H^2} + (1-u_1)\left(\frac{\alpha_H I_V}{N_H} + \frac{\alpha_{HB}B}{K+B}\right)(\lambda_1-\lambda_2) + \theta_H\lambda_1\\
\frac{d\lambda_2}{dt} &= \frac{(1-u_1)\alpha_H I_V S_H(\lambda_2-\lambda_1)}{N_H^2} + (\gamma+\theta_H)\lambda_2 - \gamma\lambda_3\\
\frac{d\lambda_3}{dt} &= -a_1 + \frac{(1-u_1)\alpha_H I_V S_H(\lambda_2-\lambda_1)}{N_H^2} + (\sigma+\delta_H+\theta_H)\lambda_3 - \sigma\lambda_4 - \omega_2\lambda_{10}\\
\frac{d\lambda_4}{dt} &= \frac{(1-u_1)\alpha_H I_V S_H(\lambda_2-\lambda_1)}{N_H^2} + (\varepsilon+\phi\delta_H+\theta_H)\lambda_4 - \varepsilon\lambda_5\\
\frac{d\lambda_5}{dt} &= \frac{(1-u_1)\alpha_H I_V S_H(\lambda_2-\lambda_1)}{N_H^2} - \rho_H\lambda_1 + (\rho_H+\theta_H)\lambda_5\\
\frac{d\lambda_6}{dt} &= -a_2 + \frac{\alpha_V I_V S_V(\lambda_7-\lambda_6)}{N_V^2} + \left(\frac{\alpha_V I_V}{N_V} + \frac{\alpha_{VB}B}{K+B}\right)(\lambda_6-\lambda_7) + (u_2+\theta_V)\lambda_6 - u_2\lambda_9\\
\frac{d\lambda_7}{dt} &= -a_2 + \frac{\alpha_V I_V S_V(\lambda_7-\lambda_6)}{N_V^2} + (\psi+\theta_V)\lambda_7 - \psi\lambda_8\\
\frac{d\lambda_8}{dt} &= -a_2 + \frac{(1-u_1)\alpha_H S_H(\lambda_1-\lambda_2)}{N_H} + \left(\frac{\alpha_V}{N_V} - \frac{\alpha_V I_V}{N_V^2}\right)S_V(\lambda_6-\lambda_7) + (\tau+\delta_V+\theta_V+u_2)\lambda_8\\
&\quad - (\tau+u_2)\lambda_9 - \omega_1\lambda_{10}\\
\frac{d\lambda_9}{dt} &= -a_2 + \frac{\alpha_V I_V S_V(\lambda_7-\lambda_6)}{N_V^2} - \rho_V\lambda_6 + (\rho_V+\theta_V)\lambda_9\\
\frac{d\lambda_{10}}{dt} &= -a_3 + (1-u_1)\left(\frac{\alpha_{HB}}{K+B} - \frac{\alpha_{HB}B}{(K+B)^2}\right)S_H(\lambda_1-\lambda_2) + (u_3+\theta_B)\lambda_{10} +\\
&\quad \left(\frac{\alpha_{VB}}{K+B} - \frac{\alpha_{VB}B}{(K+B)^2}\right)S_V(\lambda_6-\lambda_7),
\end{aligned}
\tag{30}
$$

with transerversality conditions

$$
\lambda_i(t_f) = 0, \quad i = 1, 2, 3, \ldots, 10. \tag{31}
$$

The following characterization holds;

$$
\begin{aligned}
u_1^*(t) &= \max\left\{0, \min\left(1, \frac{1}{b_1}\left(\frac{\alpha_H I_V}{N_H} + \frac{\alpha_{HB}B}{K+B}\right)S_H(\lambda_2-\lambda_1)\right)\right\}\\
u_2^*(t) &= \max\left\{0, \min\left(1, \frac{1}{b_2}\left(S_V\lambda_6 + I_V\lambda_8 - (S_V+I_V)\lambda_9\right)\right)\right\}\\
u_3^*(t) &= \max\left\{0, \min\left(1, \frac{B\lambda_{10}}{b_3}\right)\right\}
\end{aligned}
\tag{32}
$$

Preposition 1 *Corollary 4.2 of (Fleming and Rashel 1975 gives the existence of an optimal control sets $(u_1(t), u_2(t)$, and $u_3(t))$ due to the convexity of the integrand of J with respect of*

($u_1(t)$, $u_2(t)$, *and* $u_3(t)$), *a prior boundedness of the state solutions, and the local Lipschitz property of the model* (25) *with respect to the variables.*

Proof Using the Pontryagin's Maximum Principles, we obtained

$$\begin{aligned}
\frac{d\lambda_1}{dt} &= -\frac{\partial \mathcal{H}}{\partial S_H}, \quad \lambda_1(t_f) = 0,\\
\frac{d\lambda_2}{dt} &= -\frac{\partial \mathcal{H}}{\partial E_H}, \quad \lambda_2(t_f) = 0,\\
\frac{d\lambda_3}{dt} &= -\frac{\partial \mathcal{H}}{\partial I_H}, \quad \lambda_3(t_f) = 0,\\
\frac{d\lambda_4}{dt} &= -\frac{\partial \mathcal{H}}{\partial T_H}, \quad \lambda_4(t_f) = 0,\\
\frac{d\lambda_5}{dt} &= -\frac{\partial \mathcal{H}}{\partial R_H}, \quad \lambda_5(t_f) = 0,\\
\frac{d\lambda_6}{dt} &= -\frac{\partial \mathcal{H}}{\partial S_V}, \quad \lambda_6(t_f) = 0,\\
\frac{d\lambda_7}{dt} &= -\frac{\partial \mathcal{H}}{\partial E_V}, \quad \lambda_7(t_f) = 0,\\
\frac{d\lambda_8}{dt} &= -\frac{\partial \mathcal{H}}{\partial I_V}, \quad \lambda_8(t_f) = 0,\\
\frac{d\lambda_9}{dt} &= -\frac{\partial \mathcal{H}}{\partial R_V}, \quad \lambda_9(t_f) = 0,\\
\frac{d\lambda_{10}}{dt} &= -\frac{\partial \mathcal{H}}{\partial B}, \quad \lambda_{10}(t_f) = 0,
\end{aligned} \tag{33}$$

and considering the optimality condition;

$$\frac{\partial \mathcal{H}}{\partial u_1} = 0, \frac{\partial \mathcal{H}}{\partial u_2} = 0, \quad \frac{\partial \mathcal{H}}{\partial u_3} = 0 \tag{34}$$

This optimal control sets($u_1(t)$, $u_2(t)$, and $u_3(t)$) can be solved for subject to the state variables. Taking into account the bounds on the controls, the characterization can be solved as follows;

For the control $u_1(t)$, we have

$$\frac{\partial \mathcal{H}}{\partial u_1} = u_1 b_1 - \left(\frac{\alpha_H I_V}{N_H} + \frac{\alpha_{HB} B}{K+B}\right) S_H\left(\lambda_2 - \lambda_1\right) = 0$$

so that

$$u_1^*(t) = \frac{1}{b_1}\left(\frac{\alpha_H I_V}{N_H} + \frac{\alpha_{HB} B}{K+B}\right) S_H\left(\lambda_2 - \lambda_1\right) \tag{35}$$

For the control $u_2(t)$, we have

$$\frac{\partial \mathcal{H}}{\partial u_2} = u_2 b_2 - \left(S_V \lambda_6 + I_V \lambda_8 - \left(S_V + I_V\right)\lambda_9\right) = 0$$

we have that

$$u_2^*(t) = \frac{1}{b_2}\left(S_V \lambda_6 + I_V \lambda_8 - \left(S_V + I_V\right)\lambda_9\right) \tag{36}$$

For the control $u_3(t)$, we have

$$\frac{\partial \mathcal{H}}{\partial u_3} = u_3 b_3 - B\lambda_{10} = 0$$

thus, we obtained

$$u_3^*(t) = \frac{B\lambda_{10}}{b_3} \tag{37}$$

Clearly, the optimality conditions obtained by taking the derivatives of the Hamiltonian with respect to the controls on hold in the interior of the control set.

This end the proof. □

4.2 Numerical simulations of the optimal control model

The computational approach to determine the optimal control solution involves employing the forward-backward sweep method. Commencing with an initial conjecture for the optimal controls, the algorithm proceeds by advancing the state variables forward in time, utilizing the fourth-order Runge–Kutta method. Following this forward simulation, the state variables and the initial control hypothesis are utilized to retroactively solve the adjoint equation (30) by moving backward in time, adhering to a specified final condition. This backward time integration is accomplished through the implementation of the fourth-order Runge–Kutta method in reverse. The controls, denoted as $u_1(t)$, $u_2(t)$, and $u_3(t)$, are subsequently updated and employed to solve the state and adjoint systems anew.

This iterative process persists until a significant convergence is attained in the current state, adjoint, and control variables, as elucidated in prior studies (Lenhart and Workman 2007; Agusto and Adekunle 2014; Omede et al. 2023; Abidemi et al. 2024, 2024; Oguntolu et al. 2023; Peter et al. 2023; Ojo et al. 2022; Abioye et al. 2021; Peter et al. 2021; Ayoola et al. 2021; Peter et al. 2020, 2020). The parameter values utilized for the numerical illustration specifically include $\alpha_{HB} = 0.005$, while the values for the remaining parameters align with those delineated in Table 3.

4.2.1 Strategy A: Control with (u_1)

4.2.2 Strategy B: Control with (u_2)

4.2.3 Strategy C: Control with (u_3)

4.2.4 Strategy D: Combination of all the control strategy (u_1, u_2, u_3)

4.3 Discussion of results

Figure 5 depicts the simulation of the effect of the control $u_1^*(t)$ on the infected human compartment (I_H), infected animal compartment (I_V), and the bacteria population (B).

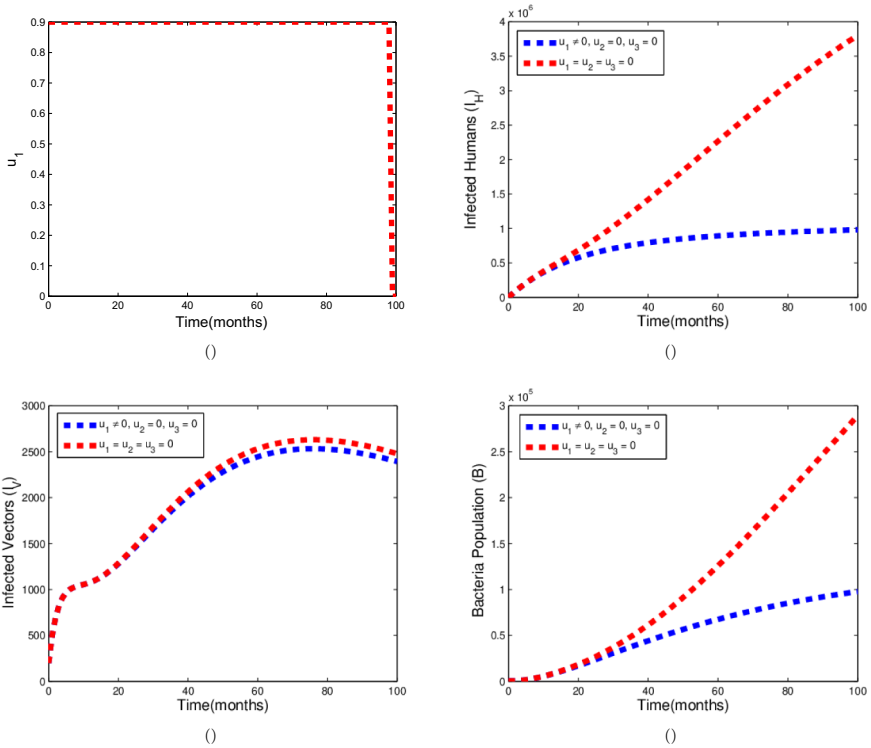

Fig. 5 Simulation of the (a) Control profile u_1 (b) Effect of u_1 on infected humans. (c) Effect of u_1 on infected animals (d) Effect of u_1 on the bacteria population

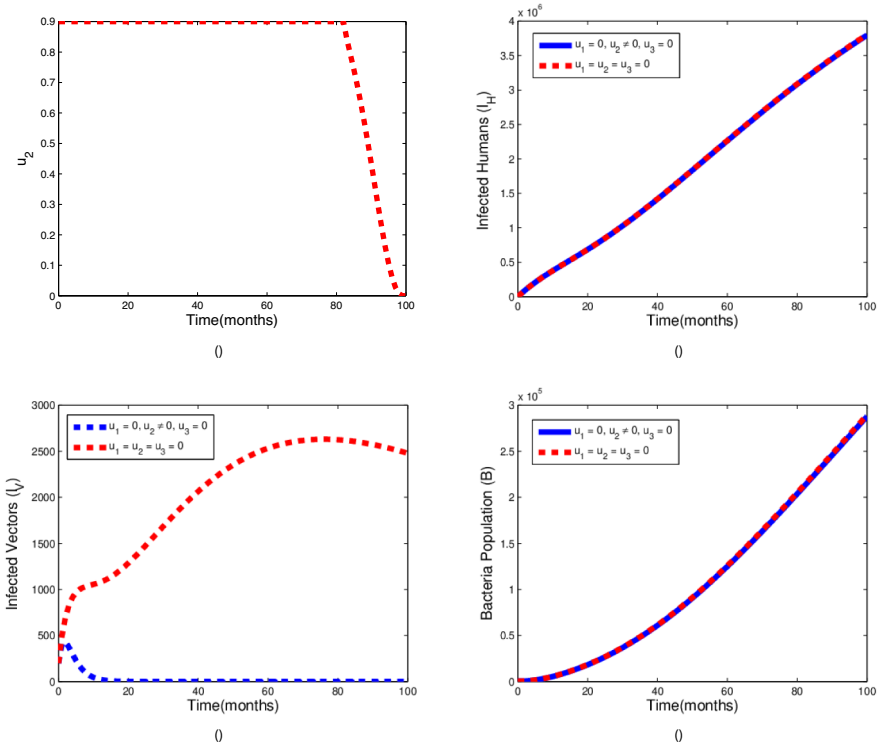

Fig. 6 Simulation of the **a** Control profile u_2 **b** Effect of u_2 on infected humans. **c** Effect of u_2 on infected animals, **d** Effect of u_2 on the bacteria population

It is observed that in the control $u_1^*(t)$ is applied, the number of infected humans reduces tremendously within 20 months. It is also observed that there is a very minimal decrease in the number of animals when the control $u_1^*(t)$ is applied. Furthermore, the bacteria population experiences a significant decrease within 40 months when the control $u_1^*(t)$ is applied.

Figure 6 depicts the simulation of the effect of the control $u_2^*(t)$ on the infected human compartment (I_H), infected animal compartment (I_V), and the bacteria population (B). It is observed that in the presence of the control $u_2^*(t)$, there is a significant decrease in the number of infected animals. Furthermore, the infected animals reduces to below 500 within 10 months. In contrast to the animal population, the presence of the control $u_2^*(t)$ has no impact on the number of infected humans and the bacteria population.

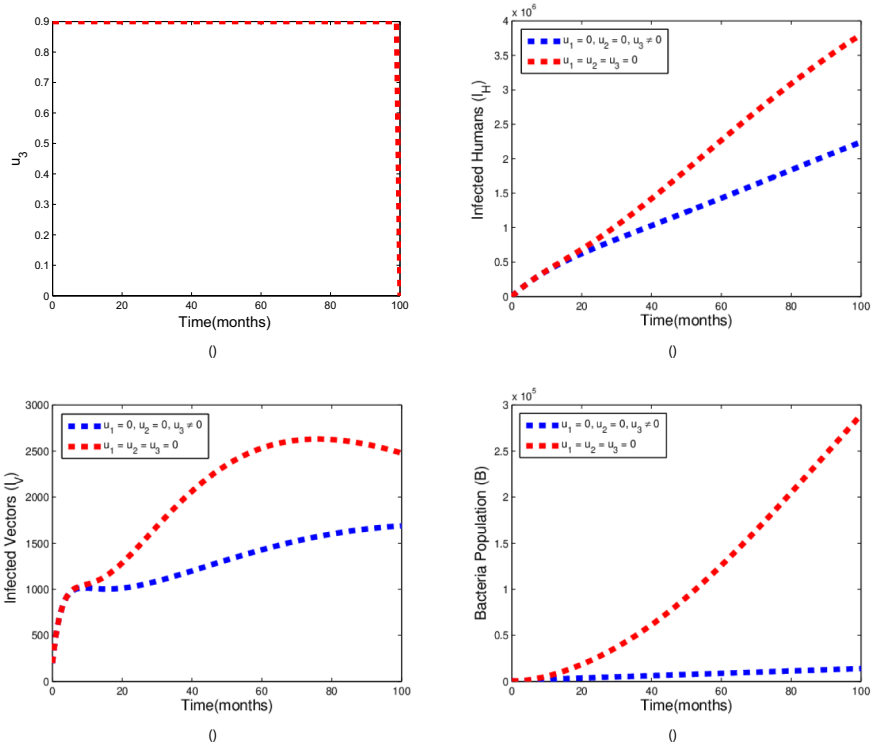

Fig. 7 Simulation of the **a** Control profile u_3, **b** Effect of u_3 on infected humans. **c** Effect of u_3 on infected animals, **d** Effect of u_3 on the bacteria population

Figure 7 depicts the simulation of the effect of the control $u_3^*(t)$ on the infected human compartment (I_H), infected animal compartment (I_V), and the bacteria population (B). It is observed that when only the control $u_3^*(t)$ is applied, the number of infected animals reduces from above 2500 to below 1500 within 40 months. It was also observed that there is a significant decrease in the number of infected humans as well as the bacteria population when only the control $u_3^*(t)$ is applied.

Figure 8 is the simulation of the effect of the combination of the controls $u_1^*(t)$, $u_2^*(t)$, and $u_3^*(t)$ on the infected human compartment (I_H), infected animal compartment (I_V), and the bacteria population (B). It is observed that when the control sets $u_1^*(t)$, $u_2^*(t)$, and $u_3^*(t)$ are applied together, it leads to a significant decline in the number of infected humans, infected animals, and the bacteria population within a very short period of time as compared to when these controls are applied separately.

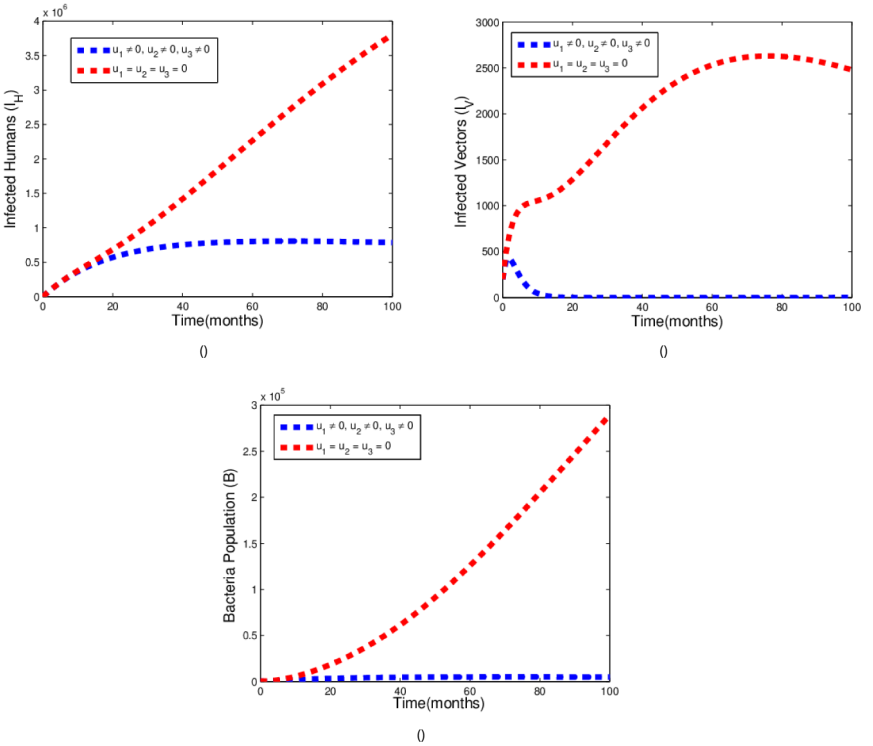

Fig. 8 Simulation of the **a** Control profile u_3, **b** Effect of u_3 on infected humans. **c** Effect of u_3 on infected animals **d** Effect of u_3 on the bacteria population

5 Conclusion

The paper introduces and extensively analyzes a deterministic mathematical model for the transmission dynamics of leptospirosis in both human and animal populations. The initial focus involves determining the basic reproduction number of the Leptospirosis model, followed by a comprehensive assessment of the local stability of the disease-free equilibrium. The study reveals that the leptospirosis model exhibits global stability in its disease-free equilibrium when the reproduction number is less than one. The application of the center manifold theory illustrates the occurrence of forward bifurcation in the Leptospirosis model. Subsequently, a sensitivity analysis on the basic reproduction numbers is conducted to identify the key parameters influencing the transmission of leptospirosis. To enhance the model, three optimal control measures are incorporated: preventative actions involving the use of hand gloves and goggles during animal handling, as well as wearing rubber boots in periods of flooding or heavy rainfall ($u_1(t)$); animal vaccination ($u_2(t)$); and environmental sanitation practices ($u_3(t)$). The paper then proceeds to numerically simulate the model, providing a practical and dynamic understanding of the impact of these control measures on the transmission dynamics of leptospirosis.

The key findings of this study is as follows;

1. The disease-free equilibrium of the Leptospirosis model is locally and globally asymptotically stable whenever the Leptospirosis basic reproduction number is less than one.
2. It is shown using the center manifold theory that the Leptospirosis model exhibits forward bifurcation.
3. The result from the sensitivity analysis of the Leptospirosis basic reproduction number indicates that the top rank parameters that greatly influenced leptospirosis transmission are Effective contact rate between susceptible vectors and infected vectors (α_V), Effective contact rate between susceptible humans and infected vectors (α_H), Recruitment rate for humans (Π_H), Recruitment rate for vectors (Π_V), Effective contact rate between susceptible humans and bacteria in the environment (α_{HB}), Effective contact rate between susceptible vectors and bacteria in the environment (α_{VB}), Progression rate from $E_H(t)$ class to $I_H(t)$ class (γ), Progression rate from E_V class to I_V class (ψ), Rate of shedding Leptospirosis bacteria in the environment from infected vectors (ω_1), and Rate of shedding Leptospirosis bacteria in the environment from infected humanss (ω_2).
4. The results from the numerical simulation revealed that the vaccination of animal control strategy ($u_2^*(t)$) alone, has no effect on the number of infected humans as well as the bacteria population. But a combined strategy of ($u_1^*(t)$),($u_2^*(t)$), and ($u_3^*(t)$) have a significant impact on reducing the number of infected humans, number of infected animals, and the bacteria population within a short period of time.

Based on the findings of this study, the following recommendations are provided for policymakers in the healthcare sector to effectively address and curb the spread of leptospirosis:

1. Integrated Control Strategies: Implement comprehensive and integrated control strategies that combine multiple measures. A combination of preventative actions ($u_1(t)$), animal vaccination ($u_2(t)$), and environmental sanitation ($u_3^*(t)$) has been shown to be significantly more effective in reducing infections.
2. Public Awareness Campaigns: Launch public awareness campaigns to educate communities about the importance of adopting preventive actions. Emphasize the use of hand gloves, goggles, and other protective measures when handling animals, especially during flooding or heavy rainfall.
3. Animal Vaccination Programs: Enhance and promote animal vaccination programs, as the results suggest that vaccination of animals alone may not be sufficient. Encourage pet owners and livestock keepers to ensure their animals are regularly vaccinated.
4. Environmental Sanitation Initiatives: Strengthen environmental sanitation initiatives, including drainage clearing and waste management. This can contribute to reducing the environmental reservoir of the bacteria responsible for leptospirosis.

Recommendation Future research work may explore solving the model by incorporating some of the approaches outlined in the references (Tassaddiq et al. 2024; Maayah et al. 2022; Arqub and El-Ajou 2013; Abo-Hammour et al. 2013).

Appendix

$$\begin{aligned}\mathcal{G}(\lambda_V^{**}) =&\mathcal{L}_1\lambda_V^{**10} + \mathcal{L}_2\lambda_V^{**9} + \mathcal{L}_3\lambda_V^{**8} + \mathcal{L}_4\lambda_V^{**7} + \mathcal{L}_5\lambda_V^{**6} + \mathcal{L}_6\lambda_V^{**5}\\ &+ \mathcal{L}_7\lambda_V^{**4} + \mathcal{L}_8\lambda_V^{**3} + \mathcal{L}_9\lambda_V^{**2} + \mathcal{L}_{10}\lambda_V^{**} + \mathcal{L}_{11}\end{aligned} \tag{38}$$

where

$$\begin{aligned}\mathcal{L}_1 &= Z_1r_1 + Z_6r_9, \mathcal{L}_2 = Z_1r_2 + Z_2r_1 + Z_6r_{10} - Z_5r_9, \mathcal{L}_3\\ &= Z_1r_3 + Z_2r_2 + Z_3r_1 + Z_6r_{11} - Z_5r_{10} - Z_7r_9(\mathcal{R}_0^V + \mathcal{R}_0^{VB} - 1), \mathcal{L}_4\\ &= Z_1r_4 + Z_2r_3 + Z_3r_2 + Z_6r_{12} - Z_4r_1 - Z_5r_{11} - Z_7r_{10}(\mathcal{R}_0^V + \mathcal{R}_0^{VB} - 1), \mathcal{L}_5\\ &= Z_1r_5 + Z_2r_4 + Z_3r_3 - Z_4r_2 - Z_5r_{12} - Z_7r_{11}(\mathcal{R}_0^V + \mathcal{R}_0^{VB} - 1), \mathcal{L}_6\\ &= Z_1r_6 + Z_2r_5 + Z_3r_4 + Z_6r_{14} - Z_4r_3 - Z_5r_{13} - Z_7r_{12}(\mathcal{R}_0^V + \mathcal{R}_0^{VB} - 1), \mathcal{L}_7\\ &= Z_1r_7 + Z_2r_6 + Z_3r_5 + Z_6r_{15} - Z_4r_4 - Z_5r_{14} - Z_7r_{13}(\mathcal{R}_0^V + \mathcal{R}_0^{VB} - 1), \mathcal{L}_8\\ &= Z_1r_8 + Z_2r_7 + Z_3r_6 - Z_4r_5 - Z_5r_{15} - Z_6r_{16} - Z_7r_{14}(\mathcal{R}_0^V + \mathcal{R}_0^{VB} - 1), \mathcal{L}_9\\ &= Z_2r_8 + Z_3r_7 + Z_5r_{16} + Z_6r_{17} - Z_4r_6 - Z_7r_{15}(\mathcal{R}_0^V + \mathcal{R}_0^{VB} - 1), \mathcal{L}_{10}\\ &= Z_3r_8 + Z_7r_{16}(\mathcal{R}_0^V + \mathcal{R}_0^{VB} - 1) - Z_4r_7 - Z_5r_{17}, \mathcal{L}_{11}\\ &= Z_7r_{17}(1 - (\mathcal{R}_0^V + \mathcal{R}_0^{VB})) - Z_4r_8.\end{aligned}$$

With

$$\begin{aligned}r_1 &= A_1A_{14} + A_5A_{10}, r_2 = A_1A_{15} + A_2A_{14} + A_6A_{10} + A_5A_{11},\\ r_3 &= A_1A_6 + A_2A_{15} + A_3A_{14} + A_7A_{10} + A_6A_{11} + A_5A_{12},\\ r_4 &= A_1A_{17} + A_2A_{16} + A_3A_{15} - A_4A_{14} + A_8A_{10} + A_7A_{11}\\ &\quad + A_6A_{12} + A_5A_{13}, r_5 = A_2A_{17} - A_1A_{18} + A_3A_{16} - A_4A_{15}\\ &\quad - A_9A_{10} + A_8A_{11} + A_7A_{12} + A_6A_{13}, r_6 = A_3A_{17} - A_2A_{18}\\ &\quad - A_4A_{16} - A_9A_{11} + A_8A_{12} + A_7A_{13}, r_7 = A_8A_{13} - A_9A_{12}\\ &\quad - A_4A_{17} - A_3A_{18}, r_8 = A_4A_{18} - A_9A_{13},\\ r_9 &= A_5A_{14}, r_{10} = A_5A_{15} + A_6A_{14}, r_{11} = A_5A_{16} + A_6A_{15} + A_7A_{14},\\ r_{12} &= A_5A_{17} + A_6A_{16} + A_7A_{15} + A_8A_{14},\\ r_{13} &= A_6A_{17} - A_5A_{18} + A_7A_{16} + A_8A_{15} - A_9A_{14},\\ r_{14} &= A_7A_{17} - A_6A_{18} + A_8A_{16} - A_9A_{15},\\ r_{15} &= A_8A_{17} - A_7A_{18} - A_9A_{16}, r_{16} = A_8A_{18} + A_9A_{17}, r_{17} = A_9A_{18},\end{aligned}$$

where

$$
\begin{aligned}
&A_1 = \alpha_H \psi g_7 (U_4 Z_1 - U_2 Z_6), A_2 = \alpha_H \psi g_7 (U_2 Z_5 + U_4 Z_2),\\
&A_3 = \alpha_H \psi g_7 (U_2 Z_7 (\mathcal{R}_0^V + \mathcal{R}_0^{VB} - 1) + U_4 Z_3),\\
&A_4 = \alpha_H \psi g_7 U_4 Z_4, A_5 = U_7 (U_3 Z_1 - U_1 Z_6),\\
&A_6 = U_3 U_7 Z_2 + U_1 U_7 Z_5 + U_3 U_8 Z_1 - U_1 U_8 Z_6,\\
&A_7 = U_3 U_7 Z_3 + U_1 U_7 Z_7 (\mathcal{R}_0^V + \mathcal{R}_0^{VB} - 1) + U_3 U_8 Z_2\\
&\quad + U_1 U_8 Z_5, A_8 = U_3 (U_8 Z_3 - U_7 Z_4) + U_1 U_8 Z_7 (\mathcal{R}_0^V + \mathcal{R}_0^{VB} - 1), A_9 = U_3 U_8 Z_4,\\
&A_{10} = \alpha_{HB} (U_4 U_9 Z_1 - (U_2 U_9 + U_7 U_{10}) Z_6),\\
&A_{11} = \alpha_{HB} (U_4 U_9 Z_2 + (U_2 U_9 + U_7 U_{10}) Z_5 - U_8 U_{10} Z_6),\\
&A_{12} = \alpha_{HB} (U_4 U_9 Z_3 + (U_2 U_9 + U_7 U_{10}) (\mathcal{R}_0^V + \mathcal{R}_0^{VB} - 1) Z_7\\
&\quad + U_8 U_{10} Z_5, A_{13} = \alpha_{HB} (U_8 U_{10} Z_7 (\mathcal{R}_0^V + \mathcal{R}_0^{VB} - 1)\\
&\quad - U_4 U_9 Z_4), A_{14} = U_7 \theta_B K (U_4 Z_1 - U_2 Z_6),\\
&A_{15} = \theta_B K (U_2 (U_7 Z_5 - U_8 Z_6) + U_4 (U_7 Z_2 + U_8 Z_1)),\\
&A_{16} = \theta_B K (U_2 (U_7 Z_1 (\mathcal{R}_0^V + \mathcal{R}_0^{VB} - 1) + U_8 Z_5)\\
&\quad + U_4 (U_7 Z_3 + U_8 Z_2)), A_{17} = \theta_B K (U_4 (U_8 Z_3 - U_7 Z_4)\\
&\quad + U_2 U_8 Z_7 (\mathcal{R}_0^V + \mathcal{R}_0^{VB} - 1)), A_{18} = U_4 U_8 \theta_B K Z_4.
\end{aligned}
$$

With

$$
\begin{aligned}
&Z_1 = U_6 (U_2 U_7 \theta_B K + U_2 U_9 + U_7 U_{10}),\\
&Z_2 = U_2 U_5 (U_7 \theta_B K + U_{10} + U_9) + U_6 U_8 (U_2 \theta_B K + U_{10})\\
&\quad - \alpha_V \Pi_V \psi g_7 (U_2 U_7 \theta_B K + U_2 U_9 + U_7 U_{10})\\
&\quad - \alpha_{VB} U_6 (U_2 U_9 + U_7 U_{10}), Z_3 = U_5 U_8 (U_2 \theta_B K + U_{10})\\
&\quad - \alpha_V \Pi_V \psi g_7 U_8 (U_2 \theta_B K + U_{10}) - \alpha_{VB} (U_2 U_5 U_9 + U_5 U_7 U_{10} + U_6 U_8 U_{10}),\\
&Z_4 = \alpha_{VB} U_5 U_8 U_{10}, Z_5 = \alpha_V \Pi_V \psi g_7 U_4 (U_7 \theta_B K + U_9)\\
&\quad + \alpha_{VB} U_4 U_6 U_9 - U_4 (U_5 U_7 \theta_B K + U_5 U_9 + U_6 U_8 \theta_B K),\\
&Z_6 = U_4 U_6 (U_7 \theta_B K + U_9), Z_7 = U_4 U_5 U_8 \theta_B K,
\end{aligned}
$$

and

$$
\begin{aligned}
U_1 = \Pi_H (g_3 g_4 (\gamma + g_2) + \gamma \sigma (\varepsilon + g_4)), U_2 = g_1 g_2 g_3 g_4 - \gamma \sigma \varepsilon \rho_H,\\
U_3 = \Pi_H g_1 g_2 g_3 g_4, U_4 = \theta_H g_1 g_2 g_3 g_4,\\
U_5 = \Pi_V g_5 g_6 g_7, U_6 = \Pi_V (g_7 (\psi + g_6) + \psi \tau),\\
U_7 = g_5 g_6 g_7 - \psi \tau \rho_V, U_8 = \theta_V g_5 g_6 g_7,\\
U_9 = \Pi_V \psi \omega_1 g_7, U_{10} = \Pi_H \gamma \omega_2 g_3 g_4.
\end{aligned}
$$

Funding The authors have not disclosed any funding.

Data availability Data used to support the findings of this study are included in the article. The authors used parameter values whose sources are from the literature as shown in Table 2.

Declaration

Conflict of interest There are no conflict of interest to declare.

References

Abidemi, A., Fatmawati, Peter, O.J.: Deterministic double dose vaccination model of COVID-19 transmission dynamics-optimal control strategies with cost-effectiveness analysis. Commun. Biomath. Sci. **7**(1), 1–33 (2024)

Abidemi, A., Fatmawati, Peter, O.J.: An optimal control model for dengue dynamics with asymptomatic, isolation, and vigilant compartments. Decis. Anal. J. **10**, 100413 (2024). https://doi.org/10.1016/j.dajour.2024.100413

Abioye, A.I., Peter, O.J., Ogunseye, H.A., Oguntolu, F.A., Oshinubi, K., Ibrahim, A.A.: Mathematical model of COVID-19 in Nigeria with optimal control. Results Phys. **24**, 104598 (2021). https://doi.org/10.1016/j.rinp.2021.104598

Abo-Hammour, Z.E., Alsmadi, O., Momani, S., Abu Arqub, O.: A genetic algorithm approach for prediction of linear dynamical systems. Math. Probl. Eng. **2013**(1), 831657 (2013)

Adler, B., de la Peña Moctezuma, A.: Leptospira and leptospirosis. Vet. Microbiol. **140**(3–4), 287–296 (2010)

Adler, B.: History of leptospirosis and leptospira. In: Leptospira and leptospirosis, pp. 1–9. Springer, Berlin, Heidelberg (2014)

Agusto, F.B., Adekunle, A.I.: Optimal control of a two-strain tuberculosis-HIV/AIDS co-infection model. Biosystems **119**, 20–44 (2014)

Al-shere, T.A., Ujiie, M., Suzuki, M., Salva, E., Belo, M.C.P., Koizumi, N., Ariyoshi, K.: Outbreak of leptospirosis after flood, the Philippines, 2009. Emerg. Infect. Dis. **18**(1), 91 (2012)

Alemneh, H.T.: A co-infection model of dengue and leptospirosis diseases. Adv. Differ. Equ. **2020**(1), 664 (2020)

Antima, Banerjee, S.: Modeling the dynamics of leptospirosis in India. Sci. Rep. **13**(1), 19791 (2023)

Arqub, O.A., El-Ajou, A.: Solution of the fractional epidemic model by homotopy analysis method. J. King Saud Univ. Sci. **25**(1), 73–81 (2013)

Aslan, I.H., Baca-Carrasco, D., Lenhart, S., Velasco-Hernandez, J.X.: An age structure model with impulse actions for leptospirosis in livestock cattle. J. Biol. Syst. **29**(01), 75–105 (2021)

Aslan, İH., Lenhart, S.: A mathematical model for cost-effectiveness analysis and early detection of leptospirosis in human. JACM **6**(1), 21–31 (2020)

Ayoola, T.A., Edogbanya, H.O., Peter, O.J., Oguntolu, F.A., Oshinubi, K., Lawal, O.M.: Mathematical modelling and optimal control analysis of typhoid fever model. J. Math. Comput. Sci. **11**(6), 6666–6682 (2021). https://doi.org/10.28919/jmcs/6262

Bierque, E., Thibeaux, R., Girault, D., Soupé-Gilbert, M.E., Goarant, C.: A systematic review of Leptospira in water and soil environments. PLoS ONE **15**(1), e0227055 (2020)

Bradley, E.A., Lockaby, G.: Leptospirosis and the environment: a review and future directions. Pathogens **12**(9), 1167 (2023)

Brett-Major, D.M., Coldren, R.: Antibiotics for leptospirosis. Cochrane Datab. Syst. Rev. (2012). https://doi.org/10.1002/14651858.CD007342.pub2

CEIC data. Available at https://www.ceicdata.com/en/india/vital-statistics-birth-rate-by-states/vital-statistics-birth-rate-per-1000-population-kerala. Accessed 20 Jan 2024

Castillo-Chavez, C., Song, B.: Dynamical models of tuberculosis and their applications. Math. Biosci. Eng. **1**(2), 361–404 (2004)

Chadsuthi, S., Chalvet-Monfray, K., Kodjo, A., Wiratsudakul, A., Bicout, D.J.: Modeling of the combined dynamics of leptospirosis transmission and seroconversion in herds. Sci. Rep. **12**(1), 15620 (2022)

Charan, J., Saxena, D., Mulla, S., Yadav, P.: Antibiotics for the treatment of leptospirosis: systematic review and meta-analysis of controlled trials. Int. J. Prev. Med. **4**(5), 501 (2013)

Chatterjee, P., Bhaumik, S., Chauhan, A.S., Kakkar, M.: Protocol for developing a database of zoonotic disease research in India (DoZooRI). BMJ Open **7**(12), e017825 (2017)

Costa, F., Hagan, J.E., Calcagno, J., Kane, M., Torgerson, P., Martinez-Silveira, M.S., Ko, A.I.: Global morbidity and mortality of leptospirosis: a systematic review. PLoS Negl. Trop. Dis. **9**(9), e0003898 (2015)

Directorate of Health Services. Available at https://dhs.kerala.gov.in/data-on-communicable-diseases/. Accessed 20 Jan 2024

Van den Driessche, P., Watmough, J.: Reproduction numbers and sub-threshold endemic equilibria for compartmental models of disease transmission. Math. Biosci. **180**(1–2), 29–48 (2002)

El-Shahed, M.: Fractional order model for the spread of leptospirosis. Int. J. Math. Anal. **8**(54), 2651–2667 (2014)

Engida, H.A., Theuri, D.M., Gathungu, D., Gachohi, J., Alemneh, H.T.: A mathematical model analysis for the transmission dynamics of leptospirosis disease in human and rodent populations. Comput. Math. Methods Med. (2022). https://doi.org/10.1155/2022/1806585
Esteves, L.M., Bulhões, S.M., Branco, C.C., Carreira, T., Vieira, M.L., Gomes-Solecki, M., Mota-Vieira, L.: Diagnosis of human leptospirosis: high resolution melting analysis for direct detection of Leptospira in the early stage of the disease in a clinical setting. bioRxiv, 311142 (2018)
Evangelista, K.V., Coburn, J.: Leptospira as an emerging pathogen: a review of its biology, pathogenesis and host immune responses. Future Microbiol. **5**(9), 1413–1425 (2010)
Faisal, S.M., McDonough, S.P., Chang, Y.F.: Leptospira: invasion, pathogenesis and persistence. The pathogenic spirochetes: strategies for evasion of host immunity and persistence, pp. 143–172 (2012)
Goarant, C.: Leptospirosis: risk factors and management challenges in developing countries. Res. Rep. Trop. Med. **28**(7), 49–62 (2016)
Guernier, V., Allan, K.J., Goarant, C.: Advances and challenges in barcoding pathogenic and environmental Leptospira. Parasitology **145**(5), 595–607 (2018)
Hamond, C., Martins, G., Lilenbaum, W.: Subclinical leptospirosis may impair athletic performance in racing horses. Trop. Anim. Health Prod. **44**, 1927–1930 (2012)
Hartskeerl, R.A., Collares-Pereira, M., Ellis, W.A.: Emergence, control and re-emerging leptospirosis: dynamics of infection in the changing world. Clin. Microbiol. Infect. **17**(4), 494–501 (2011)
Hassan, T.S., Elabbasy, E.M., Matouk, A.E., Ramadan, R.A., Abdulrahman, A.T., Odinaev, I.: Routh–Hurwitz stability and quasiperiodic attractors in a fractional-order model for awareness programs: applications to COVID-19 pandemic. Discrete Dyn. Nat. Soc. (2022). https://doi.org/10.1155/2022/1939260
Hethcote, H.W.: The mathematics of infectious diseases. SIAM Rev. **42**(4), 599–653 (2000)
Ido, Y., Hoki, R., Ito, H., Wani, H.: The prophylaxis of Weil's disease (Spirochaetosis Icterohaemorrhagica). J. Exp. Med. **24**(5), 471–483 (1916)
Jose, S.A., Raja, R., Omede, B.I., Agarwal, R.P., Alzabut, J., Cao, J., Balas, V.E.: Mathematical modeling on co-infection: transmission dynamics of Zika virus and Dengue fever. Nonlinear Dyn. **111**(5), 4879–4914 (2023)
Khan, M.A., Saddiq, S.F., Islam, S., Khan, I., Shafie, S.: Dynamic behavior of leptospirosis disease with saturated incidence rate. Int. J. Appl. Comput. Math. **2**, 435–452 (2016)
Khan, M., Zaman, G., Islam, S., Chohan, M.: Optimal campaign in Leptospirosis epidemic by multiple control variables. Appl. Math. **3**, 1655–1663 (2012). https://doi.org/10.4236/am.2012.311229.
Khan, M.A., Islam, S., Khan, S.A., Khan, I., Shafie, S., Gul, T.: Prevention of Leptospirosis infected vector and human population by multiple control variables. In: Abstract and Applied Analysis (Vol. 2014). Hindawi (2014, January)
Lakshmikantham, V., Leela, S., Martynyuk, A.A.: Stability Analysis of Nonlinear Systems, pp. 249–275. M. Dekker, New York (1989)
Lenhart, S., Workman, J.T.: Optimal Control Applied to Biological Models. CRC Press, Boca Raton (2007)
Liverpool, J., Francis, S., Liverpool, C.E., Dean, G.T., Mendez, D.D.: Leptospirosis: case reports of an outbreak in Guyana. Ann. Trop. Med. Parasitol. **102**(3), 239–245 (2008)
Loureiro, A.P., Lilenbaum, W.: Genital bovine leptospirosis: a new look for an old disease. Theriogenology **141**, 41–47 (2020)
López-Robles, G., Córdova-Robles, F.N., Sandoval-Petris, E., Montalvo-Corral, M.: Leptospirosis at human–animal–environment interfaces in Latin-America: drivers, prevention, and control measures. Biotecnia **23**(3), 89–100 (2021)
Maayah, B., Moussaoui, A., Bushnaq, S., Abu Arqub, O.: The multistep Laplace optimized decomposition method for solving fractional-order coronavirus disease model (COVID-19) via the Caputo fractional approach. Demonstratio Math. **55**(1), 963–977 (2022)
McCall, J.: Genetic algorithms for modelling and optimisation. J. Comput. Appl. Math. **184**(1), 205–222 (2005)
Md-Lasim, A., Mohd-Taib, F.S., Abdul-Halim, M., Mohd-Ngesom, A.M., Nathan, S., Md-Nor, S.: Leptospirosis and coinfection: should we be concerned? Int. J. Environ. Res. Public Health **18**(17), 9411 (2021)
Minter, A., Costa, F., Khalil, H., Childs, J., Diggle, P., Ko, A.I., Begon, M.: Optimal control of rat-borne leptospirosis in an urban environment. Front. Ecol. Evol. **7**, 209 (2019)
Mori, M., Bakinahe, R., Vannoorenberghe, P., Maris, J., De Jong, E., Tignon, M., Behaeghel, I.: Reproductive disorders and leptospirosis: a case study in a mixed-species farm (cattle and swine). Vet. Sci. **4**(4), 64 (2017)
Mwachui, M.A., Crump, L., Hartskeerl, R., Zinsstag, J., Hattendorf, J.: Environmental and behavioural determinants of leptospirosis transmission: a systematic review. PLoS Negl. Trop. Dis. **9**(9), e0003843 (2015)
Narita, M., Fujitani, S., Haake, D.A., Paterson, D.L.: Leptospirosis after recreational exposure to water in the Yaeyama islands, Japan. Am. J. Trop. Med. Hyg. **73**(4), 652 (2005)

Oguntolu, F.A., Peter, O.J., Yusuf, A., Omede, B.I., Bolarin, G., Ayoola, T.A.: Mathematical model and analysis of the soil-transmitted helminth infections with optimal control. Model. Earth Syst. Environ. **10**, 883–897 (2023) https://doi.org/10.1007/s40808-023-01815-1

Oguntolu, F.A., Peter, O.J., Yusuf, A., Omede, B. I., Bolarin, G., Ayoola, T.A.: Mathematical model and analysis of the soil-transmitted helminth infections with optimal control. Model. Earth Syst. Environ. 1–15 (2023)

Ojo, M.M., Benson, T.O., Peter, O.J., Goufo, E.D.: Nonlinear optimal control strategies for a mathematical model of COVID-19 and influenza co-infection. Physica A **607**, 128173 (2022). https://doi.org/10.1016/j.physa.2022.128173

Omede, B.I., Bolaji, B., Peter, O.J., Ibrahim, A.A., Oguntolu, F.A.: Mathematical analysis on the vertical and horizontal transmission dynamics of HIV and Zika virus co-infection. Franklin Open **6**, 100064 (2023)

Omede, B.I., Odionyenma, U.B., Ibrahim, A.A., Bolaji, B.: Third wave of COVID-19: mathematical model with optimal control strategy for reducing the disease burden in Nigeria. Int. J. Dyn. Control **11**(1), 411–427 (2023)

Omede, B.I., Peter, O.J., Atokolo, W., Bolaji, B., Ayoola, T.A.: A mathematical analysis of the two-strain tuberculosis model dynamics with exogenous re-infection. Healthc. Anal. **4**, 100266 (2023)

O'Toole, S.M., Pathak, N., Toms, G.C., Gelding, S.V., Sivaprakasam, V.: Fever, jaundice and acute renal failure. Clin. Med. **15**(1), 58 (2015)

Pappas, G., Papadimitriou, P., Siozopoulou, V., Christou, L., Akritidis, N.: The globalization of leptospirosis: worldwide incidence trends. Int. J. Infect. Dis. **12**(4), 351–357 (2008)

Peter, O.J., Abioye, A.I., Oguntolu, F.A., Owolabi, T.A., Ajisope, O., Zakari, A.G., Shaba, T.G.: Modelling and optimal control analysis of Lassa fever disease. Inform. Med. Unlocked **20**, 100419 (2020). https://doi.org/10.1016/j.imu.2020.100419

Peter, O.J., Ibrahim, M.O., Edogbanya, H.O., Oguntolu, F.A., Oshinubi, K., Ibrahim, A.A., Ayoola, T.A., Lawal, J.O.: Direct and indirect transmission of typhoid fever model with optimal control. Results Phys. **27**, 104463 (2021). https://doi.org/10.1016/j.rinp.2021.104463

Peter, O.J., Madubueze, C.E., Ojo, M.M., Oguntolu, F.A., Ayoola, T.A.: Modelling and optimal control of Monkeypox with cost-effective strategies. Model. Earth Syst. Environ. **9**, 1989–2007 (2023). https://doi.org/10.1007/s40808-022-01607-z

Peter, O.J., Viriyapong, R., Oguntolu, F.A., Yosyingyong, P., Edogbanya, H.O., Ajisope, M.O.: Stability and optimal control analysis of an SCIR epidemic model. J. Math. Comput. Sci. **10**, 2722–2753 (2020). https://doi.org/10.28919/jmcs/5001

Picardeau, M.: Diagnosis and epidemiology of leptospirosis. Med. Mal. Infect. **43**(1), 1–9 (2013)

Pontryagin, L.S.: Mathematical Theory of Optimal Processes. Routledge, London (2018)

Population Census. Available at https://www.census2011.co.in/census/state/kerala.html. Accessed 20 Jan 2024

Rahman, M.H.A.A., Hairon, S.M., Hamat, R.A., Jamaluddin, T.Z.M.T., Shafei, M.N., Idris, N., Daud, A.: Leptospirosis health intervention module effect on Knowledge, attitude, belief, and practice among wet market Workers in Northeastern Malaysia: an intervention study. Int. J. Environ. Res. Public Health **15**(7), 1396 (2018)

Sadiq, S.F., Khan, M.A., Islam, S., Zaman, G., Jung, I.H., Khan, S.A.: Optimal control of an epidemic model of leptospirosis with nonlinear saturated incidences. Ann. Res. Rev. Biol. **4**(2014), 560–576 (2014)

Sykes, J.E., Haake, D.A., Gamage, C.D., Mills, W.Z., Nally, J.E.: A global one health perspective on leptospirosis in humans and animals. J. Am. Vet. Med. Assoc. **260**(13), 1589–1596 (2022)

Sykes, J.E., Reagan, K.L., Nally, J.E., Galloway, R.L., Haake, D.A.: Role of diagnostics in epidemiology, management, surveillance, and control of leptospirosis. Pathogens **11**(4), 395 (2022)

Tassaddiq, A., Qureshi, S., Soomro, A., Arqub, O.A., Senol, M.: Comparative analysis of classical and Caputo models for COVID-19 spread: vaccination and stability assessment. Fixed Point Theory Algorithms Sci. Eng. **2024**(1), 2 (2024)

Thibeaux, R., Iraola, G., Ferrés, I., Bierque, E., Girault, D., Soupé-Gilbert, M.E., et al.: Deciphering the unexplored Leptospira diversity from soils uncovers genomic evolution to virulence. Microb. Genom. **4**(1), 1–10 (2018)

Tubiana, S., Mikulski, M., Becam, J., Lacassin, F., Lefèvre, P., Gourinat, A.C., d'Ortenzio, E.: Risk factors and predictors of severe leptospirosis in New Caledonia. PLoS Negl. Trop. Dis. **7**(1), 1-10 e1991 (2013)

Urban death rates in India in 2020, by state. https://www.statista.com/statistics/616300/urban-death-rate-by-state-and-union-territory-india/

Verma, A., Soto, E., Illanes, O., Ghosh, S., Fuentealba, C.: Detection and genotyping of *Leptospira* spp. from the kidneys of a seemingly healthy pig slaughtered for human consumption. J. Infect. Dev. Ctries. **9**(05), 530–532 (2015)

Vernel-Pauillac, F., Werts, C.: Recent findings related to immune responses against leptospirosis and novel strategies to prevent infection. Microbes Infect. **20**(9–10), 578–588 (2018)
Xu, Y., Ye, Q.: Human leptospirosis vaccines in China. Hum. Vaccin. Immunother. **14**(4), 984–993 (2018)
Yaakob, Y., Rodrigues, K.F., John, D.V.: Leptospirosis: recent incidents and available diagnostics—a review. Med. J. Malays. **70**(6), 351 (2015)

Authors and Affiliations

Festus Abiodun Oguntolu[1] · Olumuyiwa James Peter[2,3] · Benjamin Idoko Omede[4] · Ghaniyyat Bolanle Balogun[5] · Tawakalt Abosede Ayoola[6]

✉ Olumuyiwa James Peter
peterjames4real@gmail.com

[1] Department of Mathematics, Federal University of Technology, Minna, Niger State, Nigeria

[2] Department of Mathematical and Computer Sciences, University of Medical Sciences, Ondo, Ondo State, Nigeria

[3] Department of Epidemiology and Biostatistics, School of Public Health, University of Medical Sciences, Ondo, Ondo State, Nigeria

[4] Department of Mathematical Sciences, Prince Abubakar Audu (Formerly Kogi State) University, Anyigba, Nigeria

[5] Department of Computer Science, University of Ilorin, Ilorin, Kwara State, Nigeria

[6] Department of Mathematical Sciences, Osun State University, Osogbo, Osun State, Nigeria